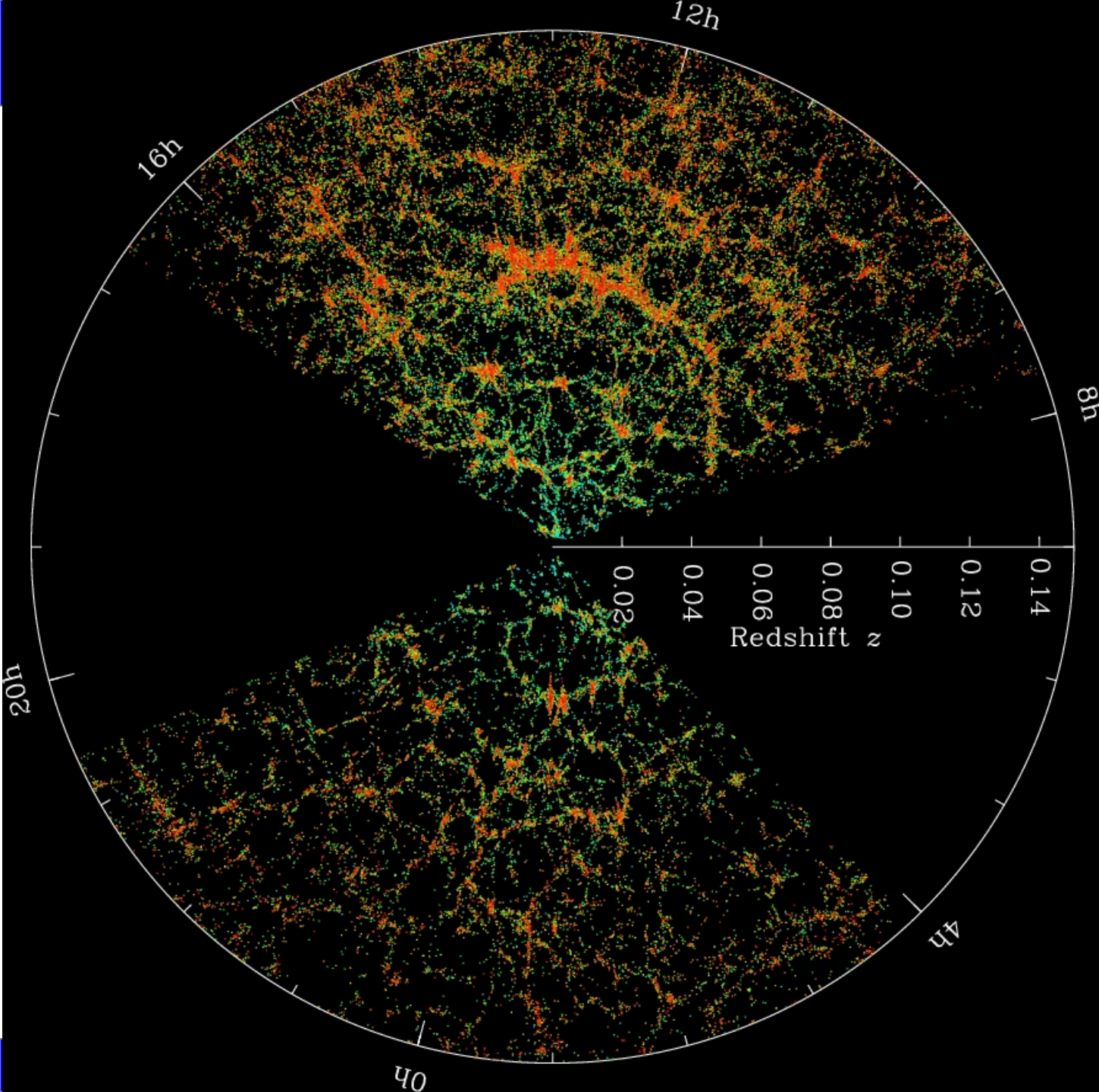


Galaxy Clusters and the IntraCluster Medium





credit: SDSS collab.

Abell 1689

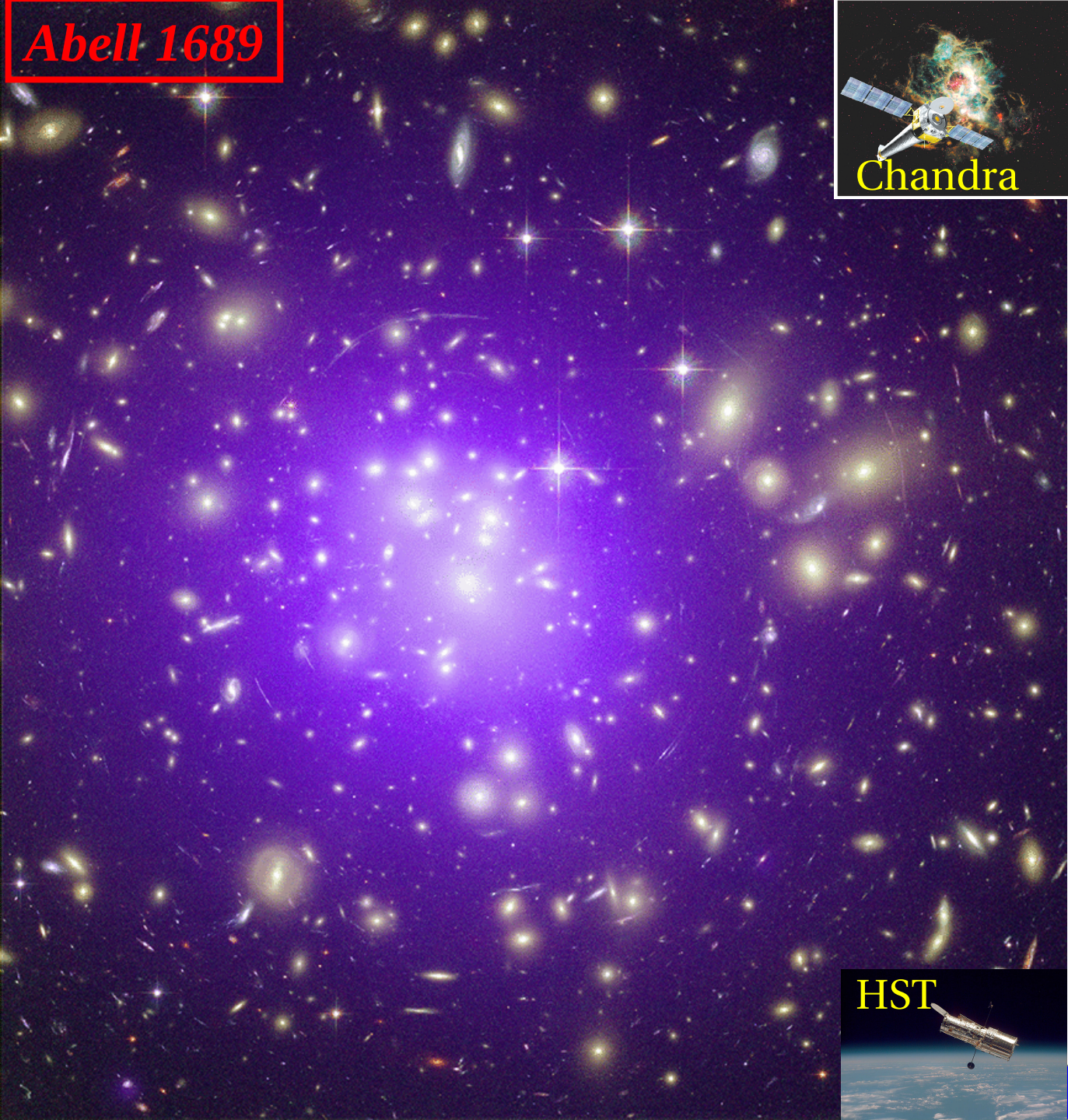
What is a galaxy cluster ?

- Concentration of $\sim 10^3$ galaxies
- $\sigma_v \sim 500-1000 \text{ km s}^{-1}$
- Size: $\sim 1-2 \text{ Mpc}$
- Mass: $\sim 10^{14} \text{ Msun}$

HST



Abell 1689



What is a galaxy cluster ?

- Concentration of $\sim 10^3$ galaxies
- $\sigma_v \sim 500-1000 \text{ km s}^{-1}$
- Size: $\sim 1-2 \text{ Mpc}$
- Mass: $\sim 10^{14} \text{ Msun}$
- ICM temperature:
 $T_x \sim 2-10 \text{ keV}$
fully ionized plasma;

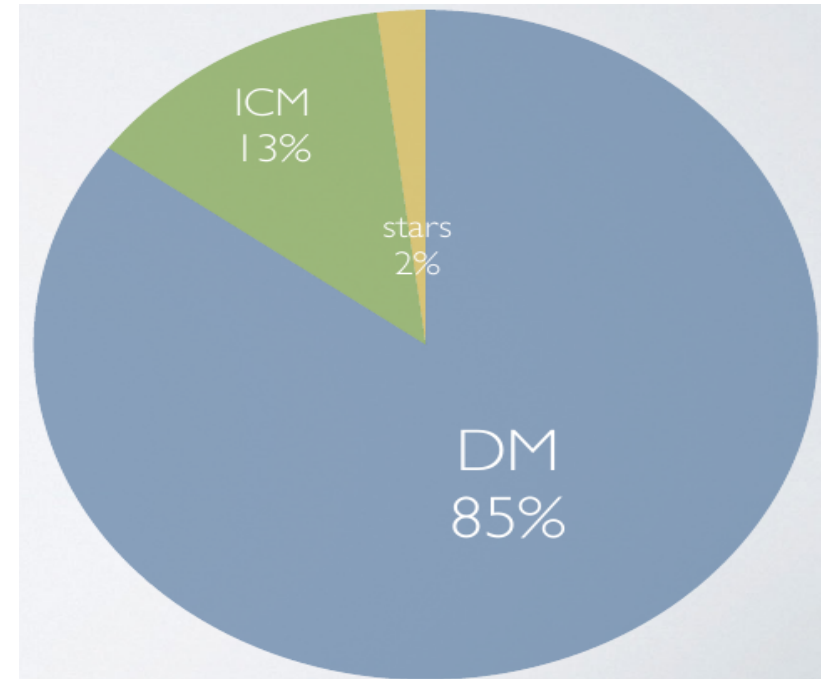


The Constituents Of Galaxy Cluster

Dark Matter: Accounts for 85% of cluster mass. Unknown collisionless particles.

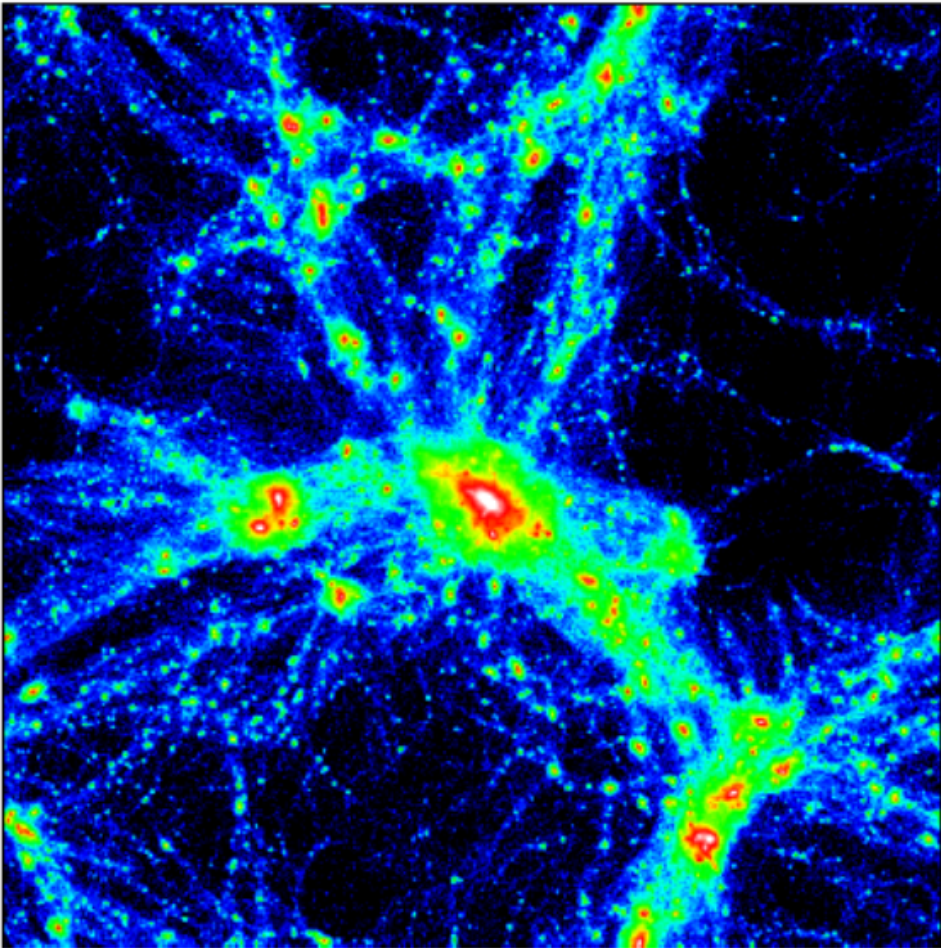
Intra-cluster medium: hot, optically thin gas. 85% of baryons. It emits X-ray radiation.

Galaxies: 100s to 1000s galaxies, 15% of baryons.

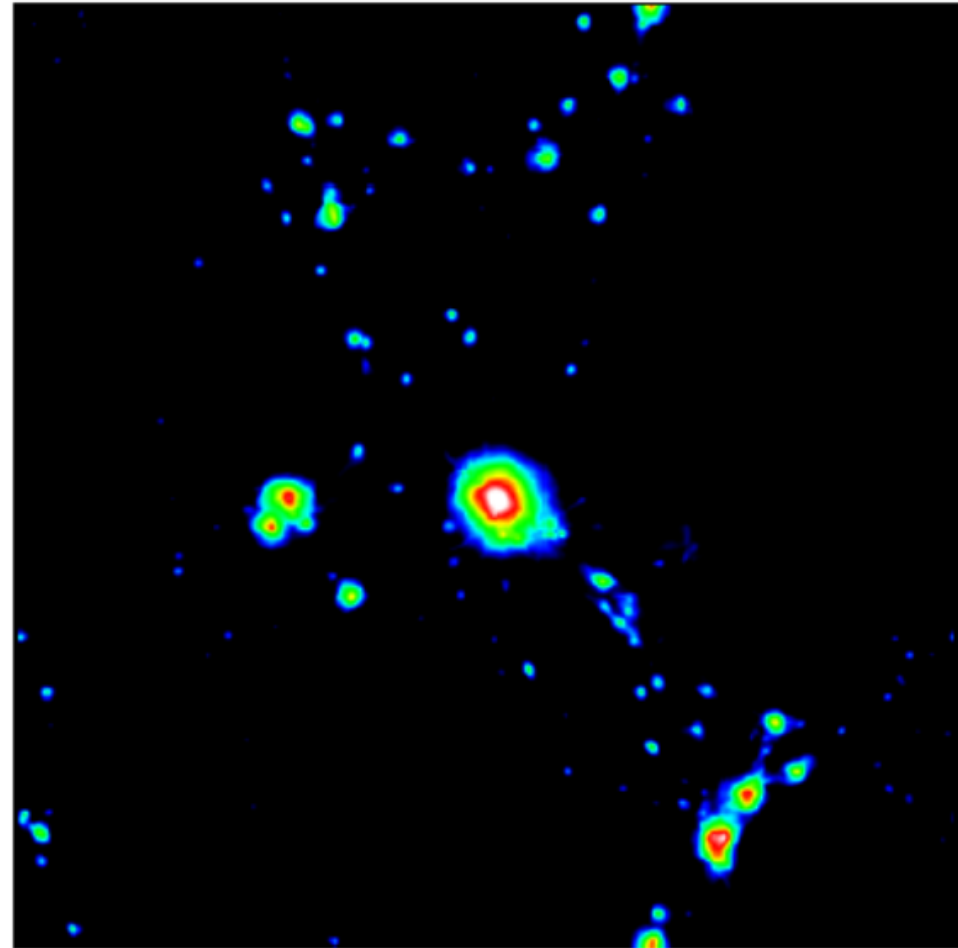


The Constituents Of Galaxy Cluster

Dark Matter



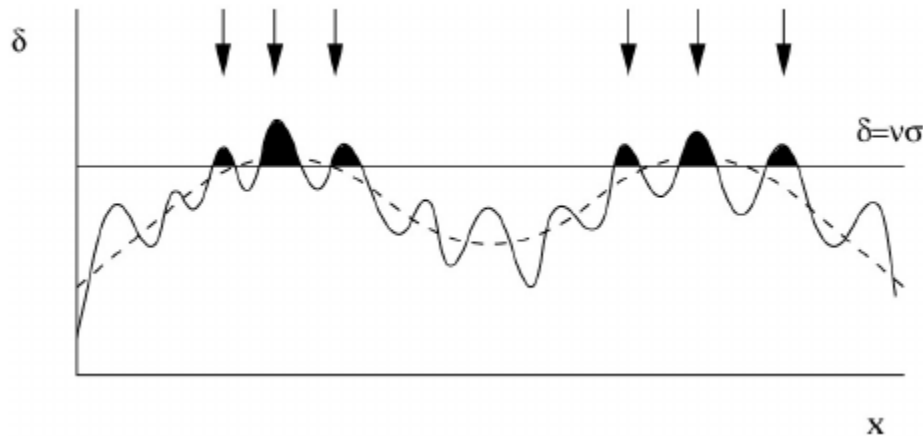
Baryons



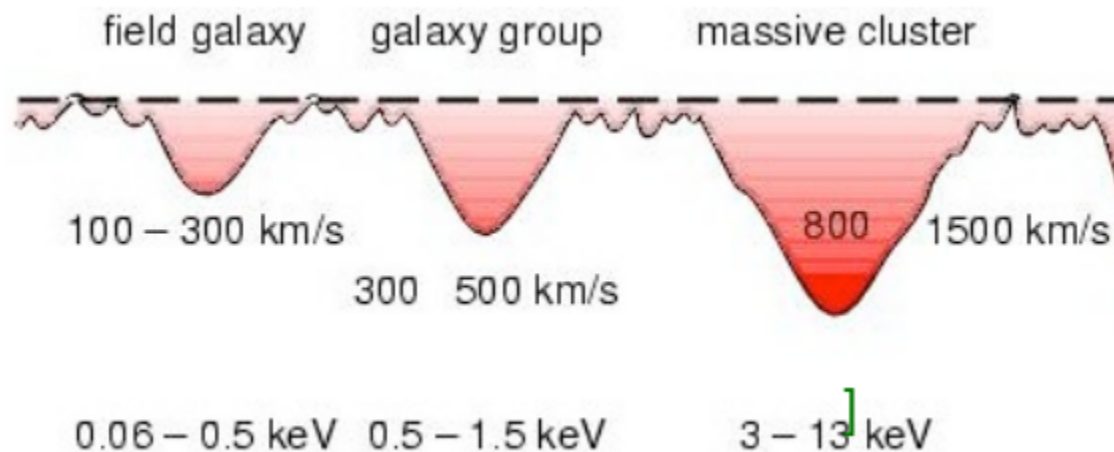
In simulations

Cluster Formation

Collapse from initial density fluctuations



The deep gravitational potential wells of clusters lock metals produced by member galaxies: the ICM is a fossil record of the chemical enrichment of the Universe



Cluster border

The cluster border is not a well-defined quantity: clusters are not closed spheres, however it is convenient to define a cluster as the mass enclosed in a radius corresponding to a fixed Δ .

Δ is defined as the density contrast with respect to the mean or the critical density of the Universe at the cluster redshift.

The critical density is the value required to have a flat Universe.

$$\rho_c \equiv 3H^2(z)/8\pi G.$$

$$M_\Delta = \frac{4\pi}{3} r_\Delta^3 \rho_{crit} \Delta_c$$

The ICM

In their formation process, galaxy clusters undergo adiabatic compression and shocks providing the primordial heat to the intracluster medium, a hot gas confined by the cluster's gravitational potential well.

Clusters are permeated by this low-density plasma, which strongly emits X-ray radiation:

- free-free: thermal bremsstrahlung → continuum
- free-bound: recombination → continuum
- bound-bound: de-excitation radiation → line emission

Mainly H, He, but with heavy elements (O, Fe, ..)

The ICM

Main emission processes: thermal Bremsstrahlung radiation and metal emission lines, proportional to the square of the gas density:

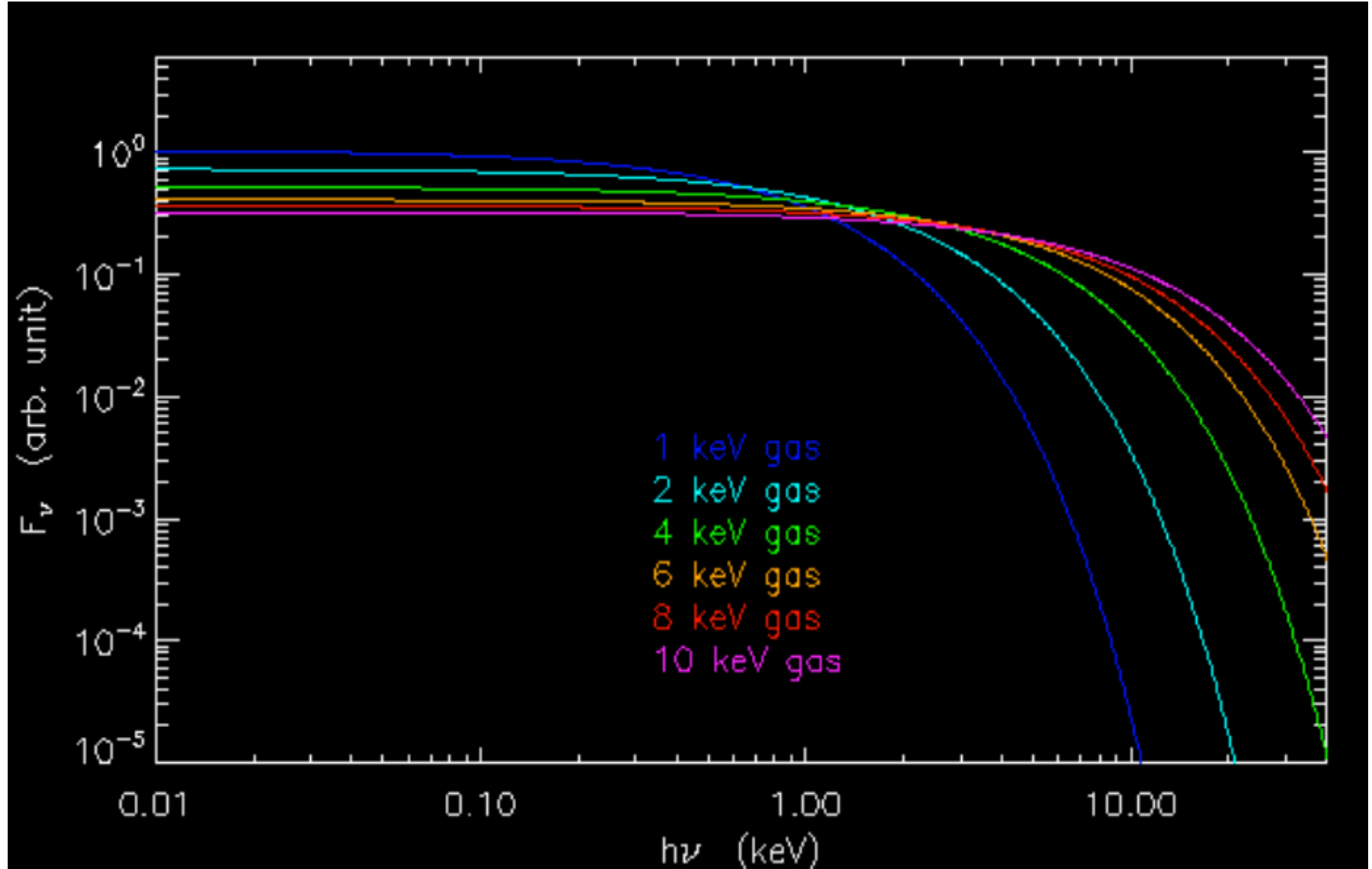
$$\epsilon_\nu = \frac{2^4 e^6}{3 m_e \hbar c^2} \left(\frac{2\pi k_B T}{m_e c^2} \right)^{1/2} \mu_e n_e^2 g(Z, T, \nu) \exp\left(\frac{h\nu}{k_B T}\right) (k_B T)^{-1}$$

Integrating ϵ_ν over the X-ray emission energy range and gas distribution,

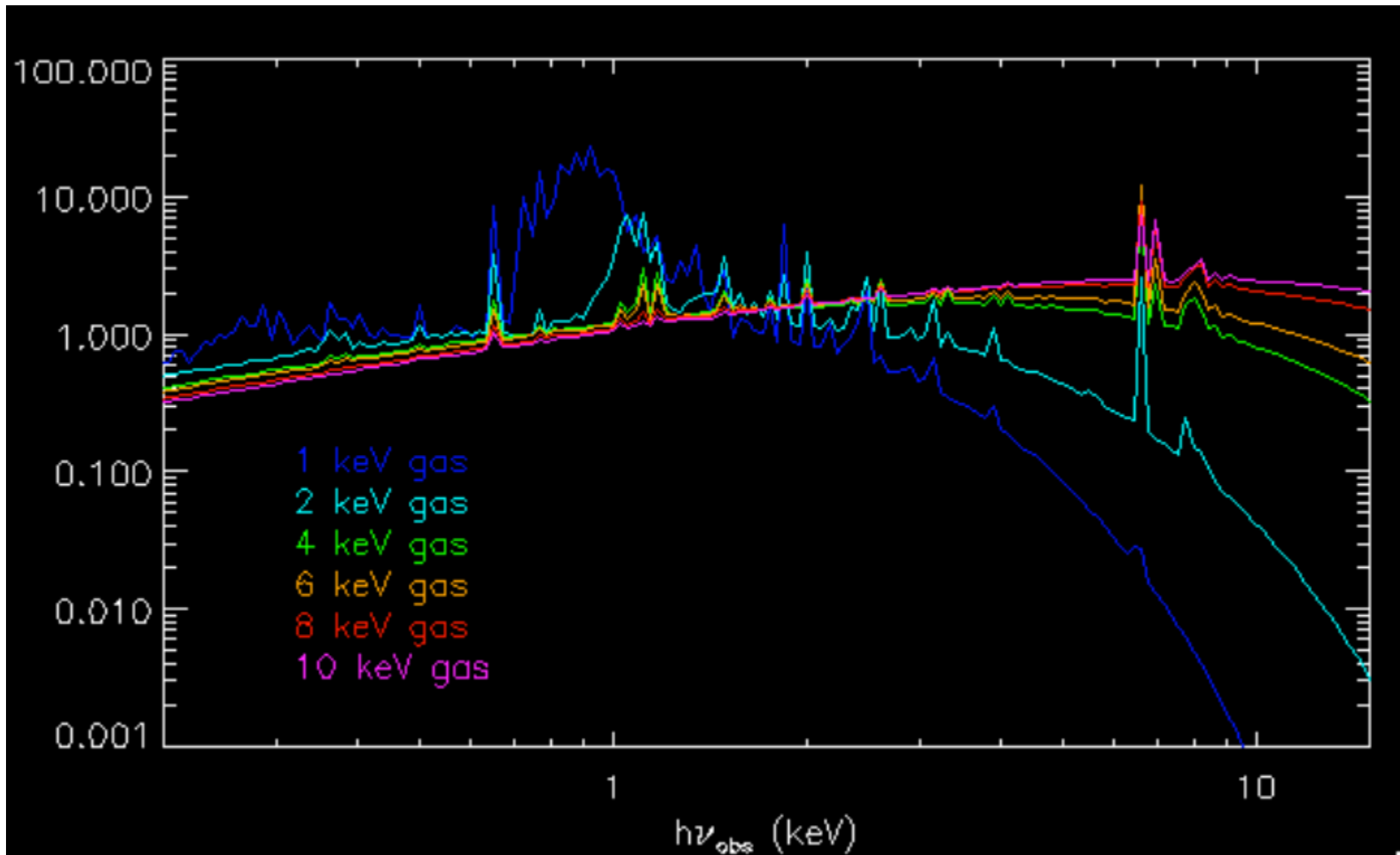
$$\epsilon_\nu \equiv \frac{dL}{dV d\nu} \quad L_x = \frac{2^4 e^6}{3 \hbar m_e c^2} \left(\frac{2\pi k T}{3 m_e c^2} \right)^{1/2} \mu_e \bar{g}(T) \int n_e^2 4\pi r^2 dr,$$

we obtain $L_X \sim 10^{43} - 10^{45}$ erg s⁻¹.

The ICM

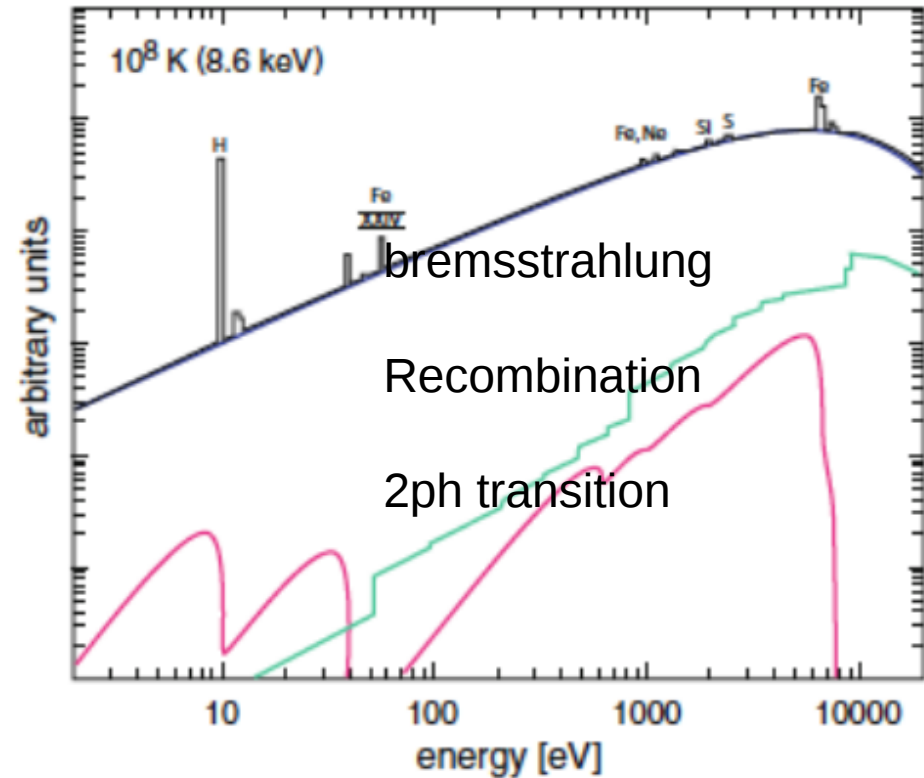
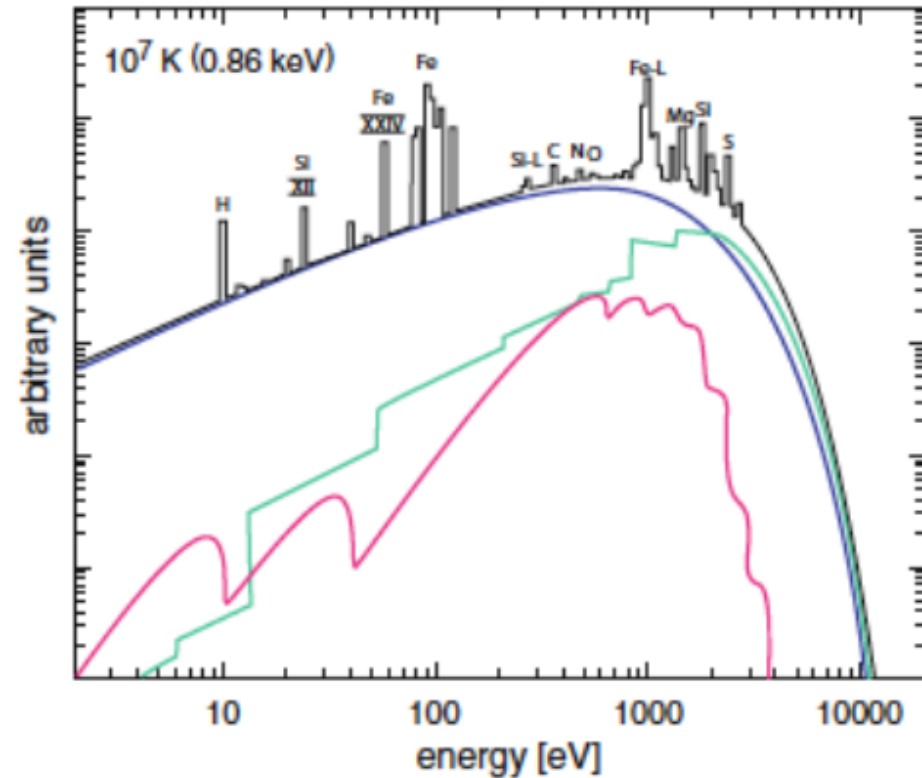


The ICM



The ICM

Plasma radiation codes to model the X-ray spectrum

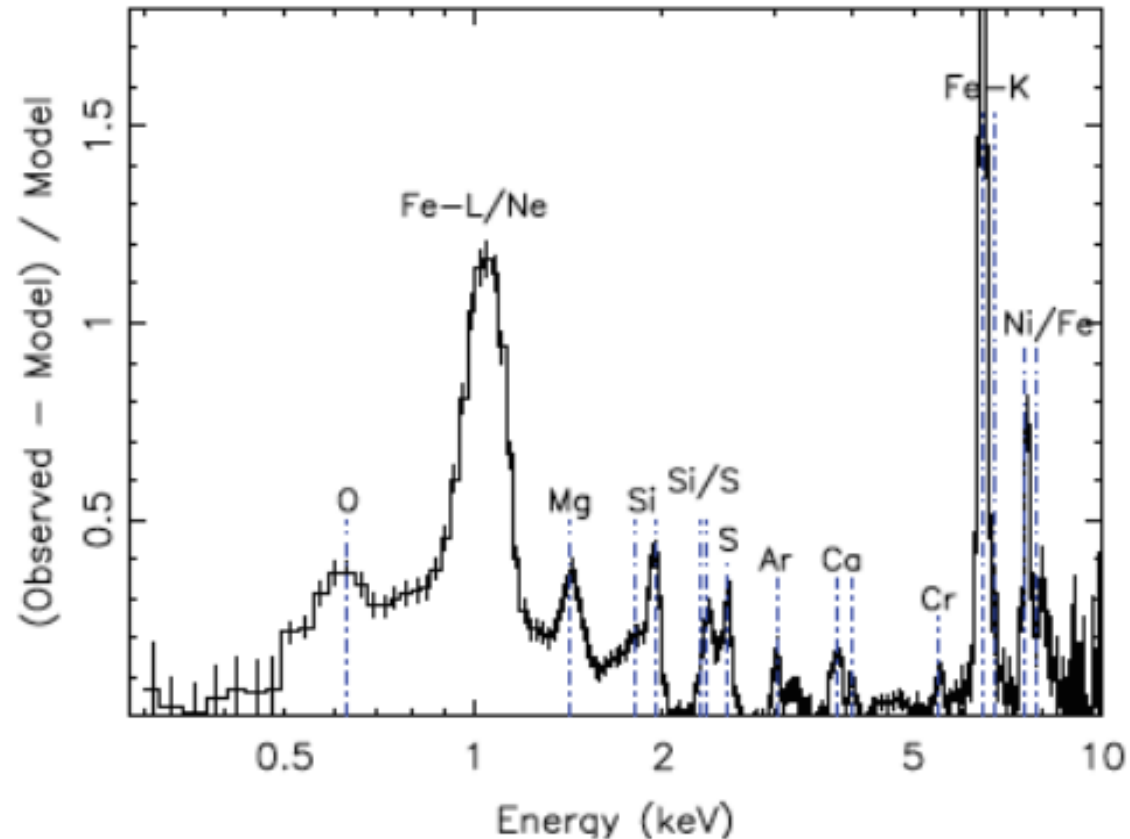


When T increases, bremsstrahlung dominates shape of continuum spectrum

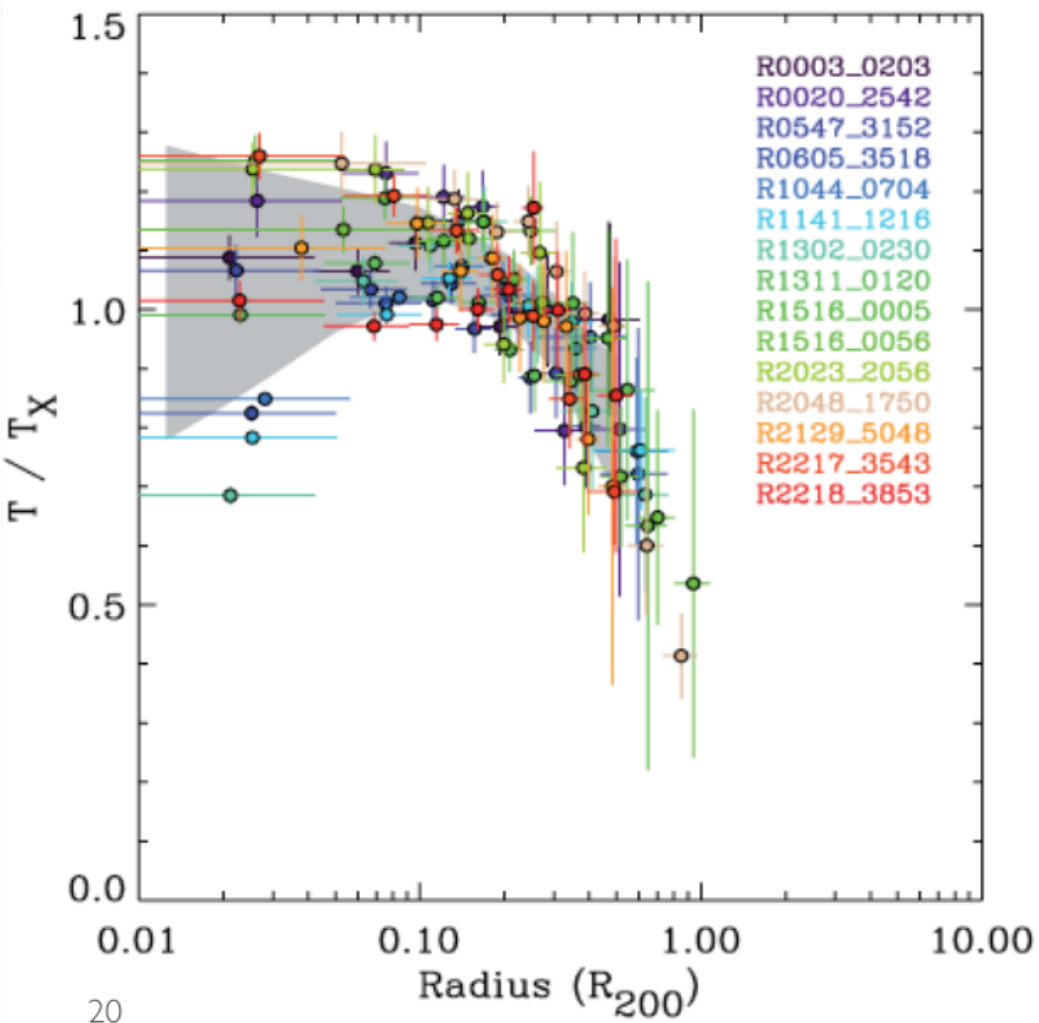
The ICM

The deep gravitational potential wells of clusters lock metals produced by member galaxies: the ICM is a fossil record of the chemical enrichment of the Universe

Most prominent signature of the metal enrichment is the Fe K-line complex at 6.7 keV (the only accessible line at high- z)



Temperature profile

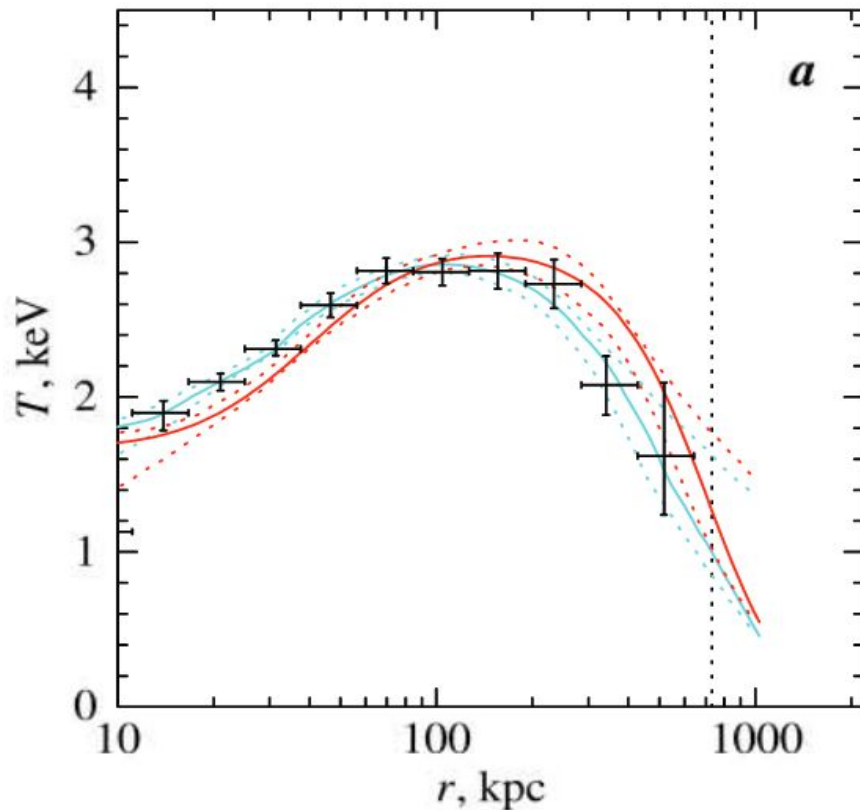


Temperature profile

Vikhlinin introduced a parametric model to describe the distribution of the ICM temperature

$$T_{3D} = T_0 \frac{(r/r_t)^{-a} (x + T_{min}/T_0)}{[1 + (r/r_t)^b]^{c/b} (x + 1)}$$

$$x = (r/r_{cool})^{a_{cool}}$$



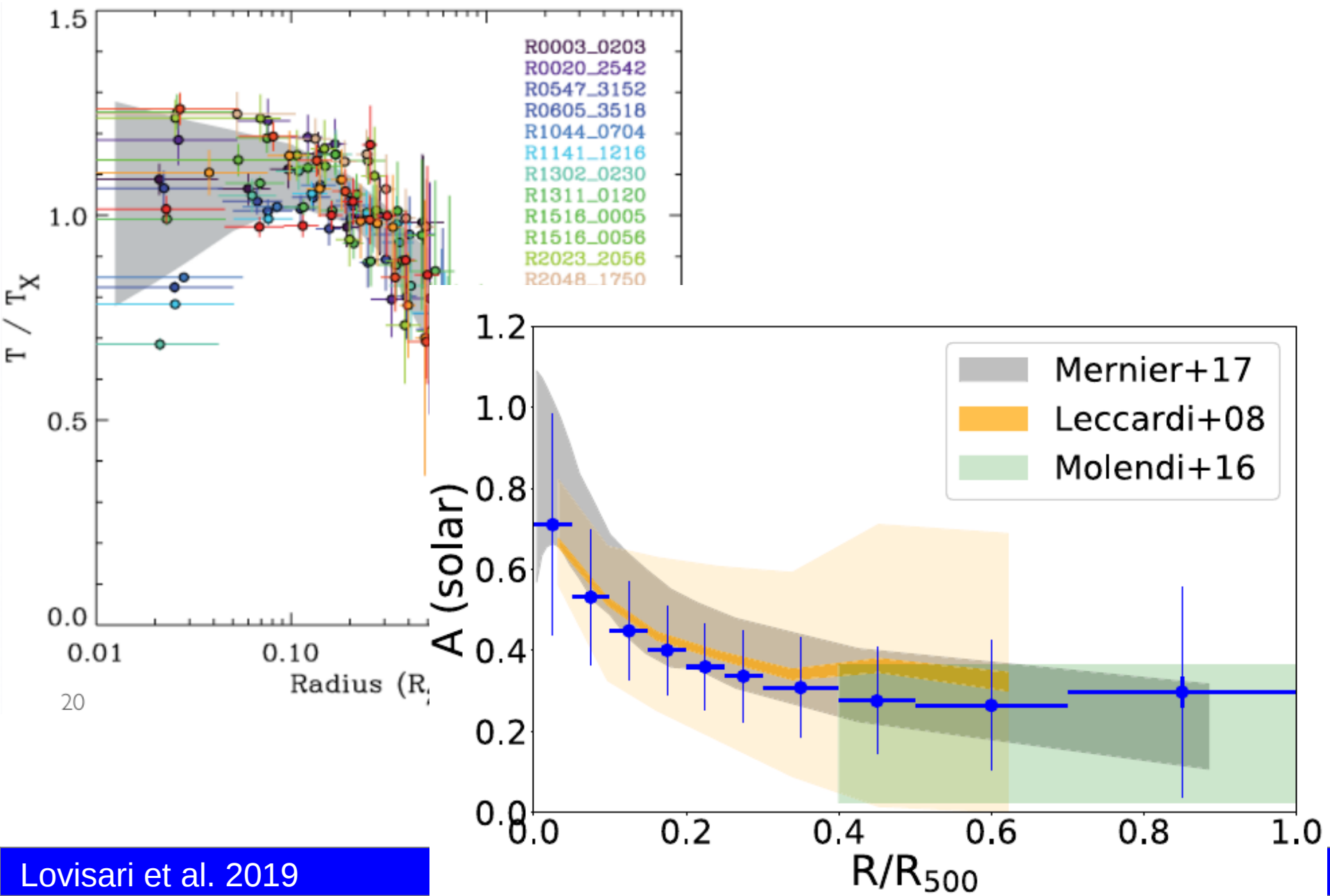
The model has a “bell” shape

Points: measured temperatures
(with Chandra spectra)

Red line: Vikhlinin 3D model

Blue line: projected 3D model
fitted to the data

Temperature profile



Hydrostatic Mass

Gravitational potential for a spherically symmetric object

$$\Phi(r) = -\frac{GM}{r}$$

Equation of state:

$$P = nkT = \frac{\rho_{gas}}{\mu m_p} kT$$

Hydrostatic Mass

Hydrostatic equilibrium: balance of gravitational and pressure forces

$$\nabla P_{gas} = -\rho_{gas} \nabla \Phi$$

Include the gravitational potential



$$\frac{dP}{dr} = -\rho_{gas} \frac{d\Phi}{dr} = -\rho_{gas} \frac{GM(r)}{r^2}$$

Include equation of state



Hydrostatic Mass:

$$M(r) = -\frac{r^2}{\rho_{gas}} \frac{dP}{dr} = -\frac{r}{G \mu m_p} \left[\frac{d \ln \rho_{gas}}{d \ln r} + \frac{d \ln T}{d \ln r} \right]$$

The β -model for the gas distribution

combining the Jeans

$$M(r) = -\frac{\sigma_r^2 r}{G} \left\{ \frac{d \ln \rho}{d \ln r} \right\}$$

and hydrostatic equilibrium eqs

$$M(r) = -\frac{kT r}{G\mu m_p} \left\{ \frac{d \ln \rho_g}{d \ln r} \right\}$$

$$\frac{\sigma_r^2 \mu m_p}{kT} \equiv \beta$$

$$\frac{\rho_g}{\rho_{g0}} = \left(\frac{\rho}{\rho_0} \right)^\beta \quad \text{Assuming a King profile for the galaxies distribution} \quad \rho = \rho_0 \left(1 + \left(\frac{r}{r_c} \right)^2 \right)^{-3/2}$$

Gas density distribution

$$\rho_g = \rho_{g0} \left(1 + \left(\frac{r}{r_c} \right)^2 \right)^{-3/2\beta}$$

Gas density profile

The shape of cluster density profiles, n_e , is affected by the individual evolution history of the cluster e.g.:

- merging phenomena
- feedbacks in the core

For this reason the Beta profile introduced by Cavaliere & Fusco Femiano based on simple physical assumptions is not adequate

Vikhlinin introduced in 2006 a parametric model to account for the variegated cluster population

$$n_p n_e = n_0^2 \frac{(r/r_c)^{-\alpha}}{(1 + r^2/r_c^2)^{3\beta - \alpha/2}} \frac{1}{(1 + r^\gamma/r_s^\gamma)^{\epsilon/\gamma}} + \frac{n_{02}^2}{(1 + r^2/r_{c2}^2)^{3\beta_2}} \cdot$$

Term for the outskirts

Term accounting for the core

Gas density profile

$$n_p n_e = n_0^2 \frac{(r/r_c)^{-\alpha}}{(1 + r^2/r_c^2)^{3\beta - \alpha/2}} \frac{1}{(1 + r^\gamma/r_s^\gamma)^{\epsilon/\gamma}} + \frac{n_{02}^2}{(1 + r^2/r_{c2}^2)^{3\beta_2}}.$$

Remember that

$$n_e = Z n_p$$

$$\rho_{gas} = m_p n_e A/Z$$

Where:

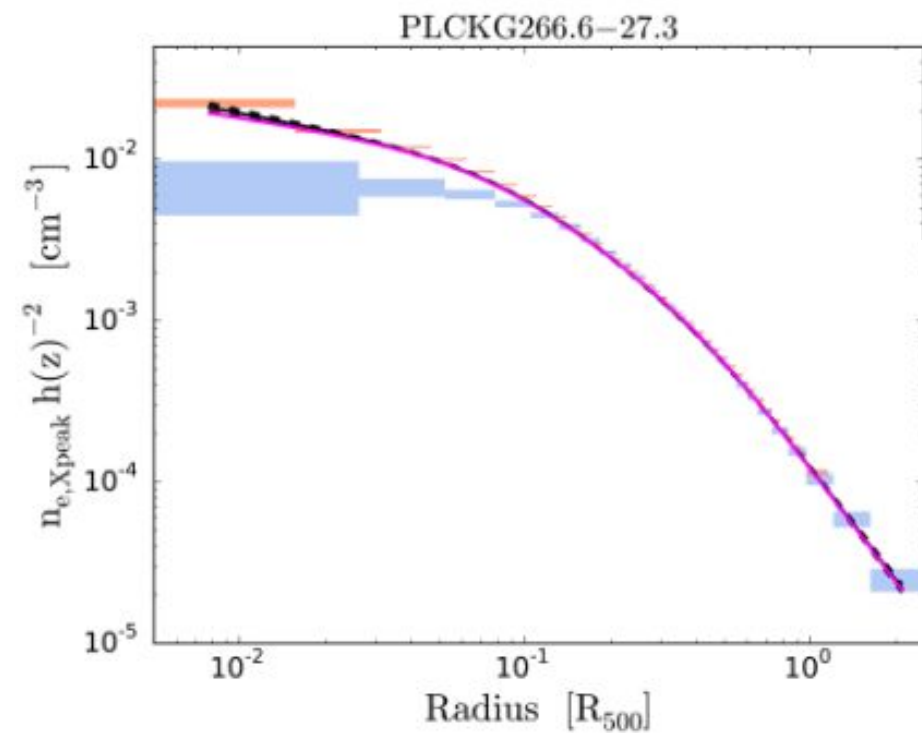
Z is the average nuclear charge

A is the average nuclear mass

Both computed under some assumptions.

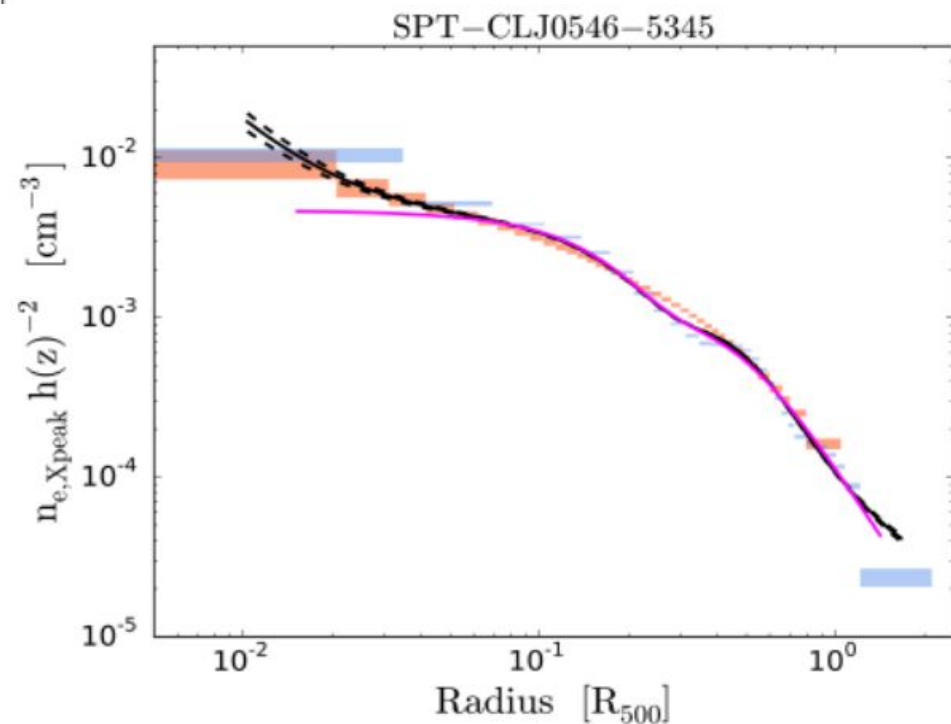
Typically A=1.4 and Z=1.2

Gas density profile



Relaxed cluster

The variegate population of clusters



Disturbed cluster

Surface brightness profile

X-ray emission $\epsilon = n_e^2 \tilde{\Lambda}(t)$

Surface brightness

$$S_x(R) = \frac{2}{4\pi} \int_R^\infty n_e^2 \tilde{\Lambda}(t) dz$$

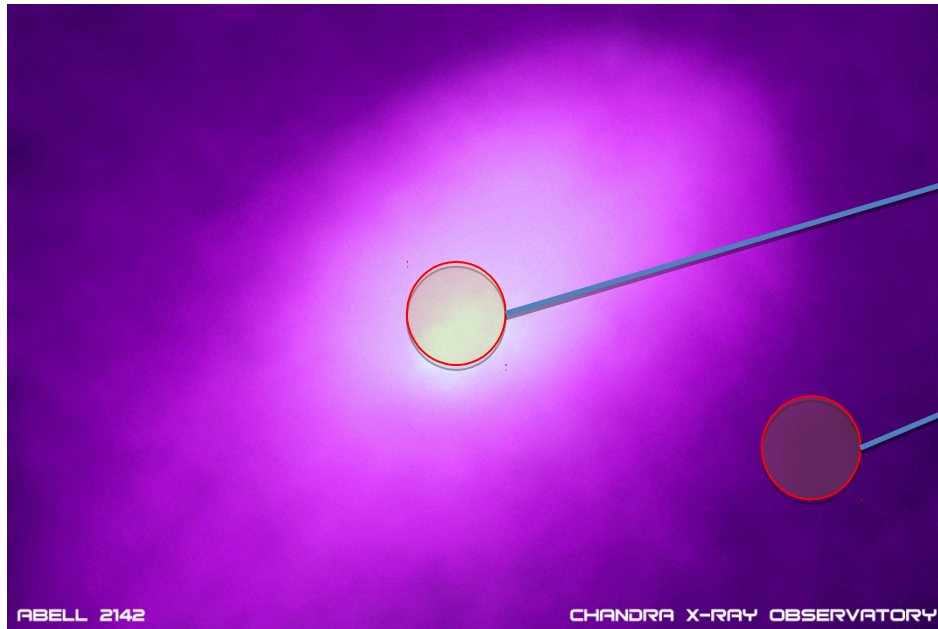
Proportional to $n_e^2 \rightarrow$ difficult to observe the cluster outskirts

In inverse proportion to $(1+z)^4 \rightarrow$ difficult to have high S/N X-ray observations at high redshift

$$S_x(R) = \frac{n_{e0}^2 \tilde{\Lambda}(t) r_c}{4\pi} \frac{\Gamma(0.5)\Gamma(3\beta - 0.5)}{\Gamma(3\beta)} \left(1 + \left(\frac{R}{r_c} \right)^2 \right)^{-3\beta+1/2} (1+z)^{-4}$$

X-ray emission

$$\epsilon(\nu) \propto n_e^2$$



$$n_e \sim 10^{-2} \text{ cm}^{-3}$$

$$n_e \sim 10^{-4} \text{ cm}^{-3}$$

X-ray emission

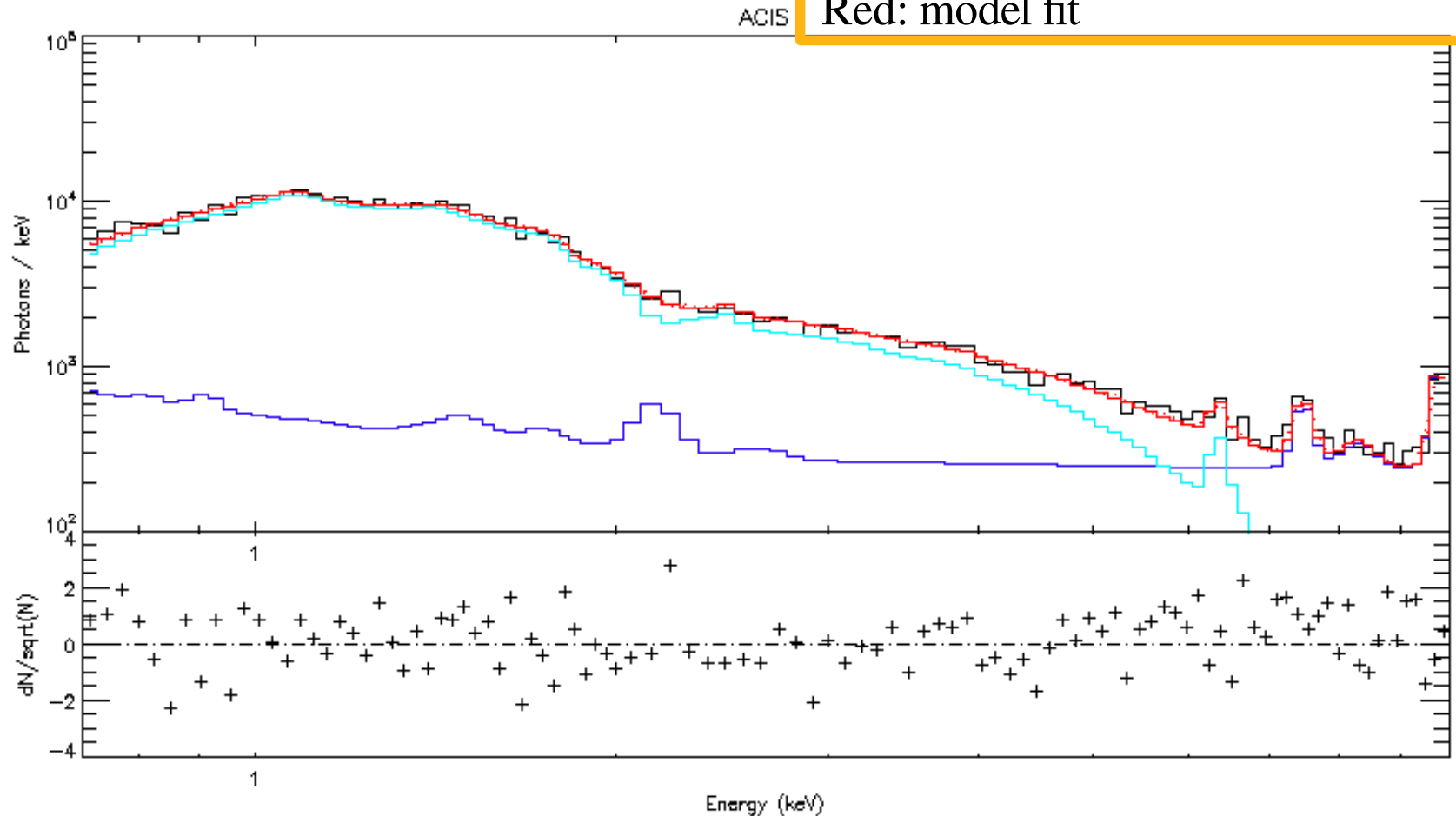
Spectrum from the center of a cluster

Black: data

Blue: background

Cyan: Bremsstrahlung + emission lines

Red: model fit



X-ray emission

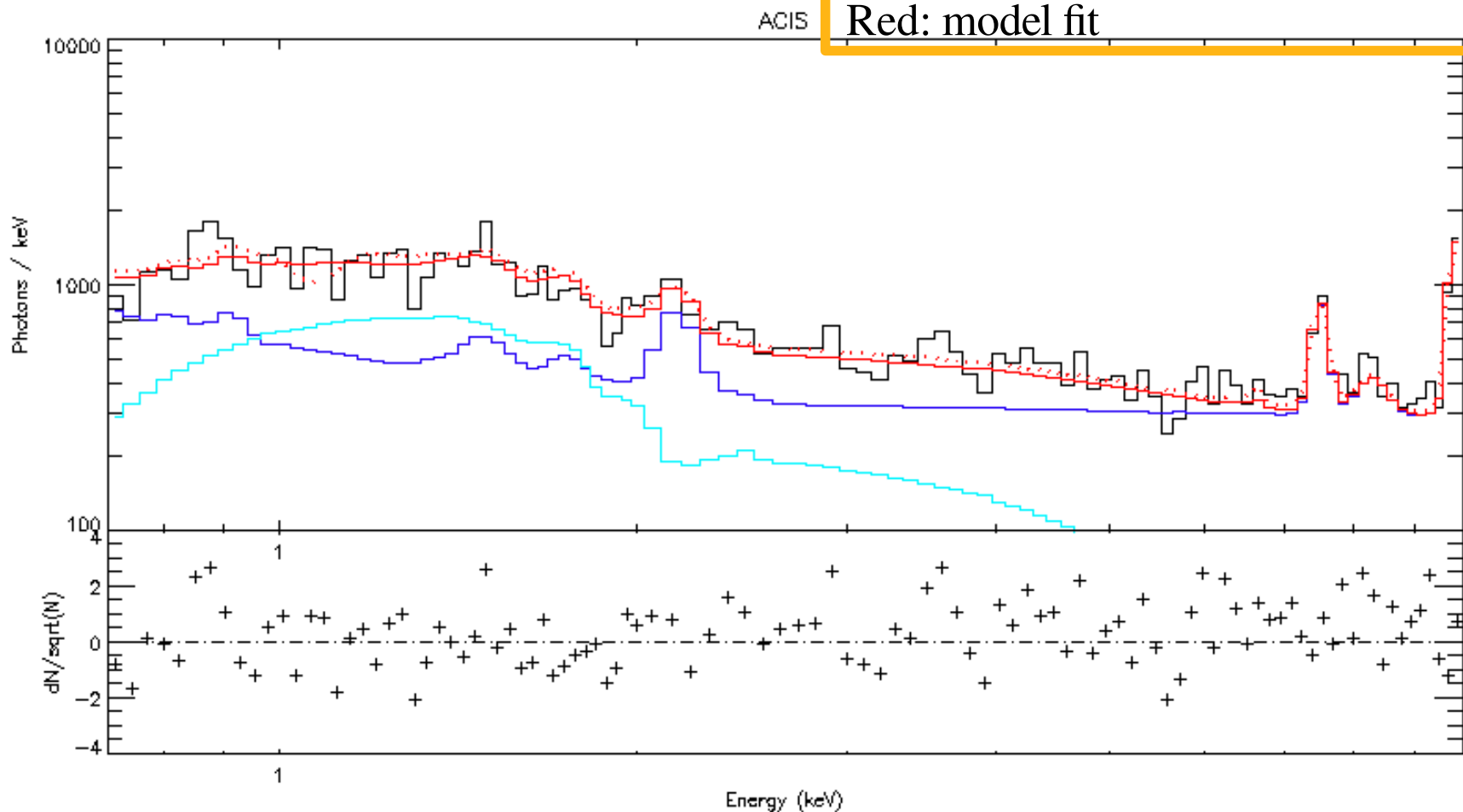
Spectrum from the outer regions of a cluster

Black: data

Blue: background

Cyan: Bremsstrahlung + emission lines

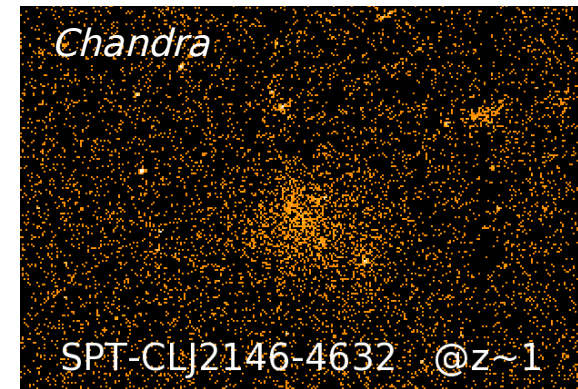
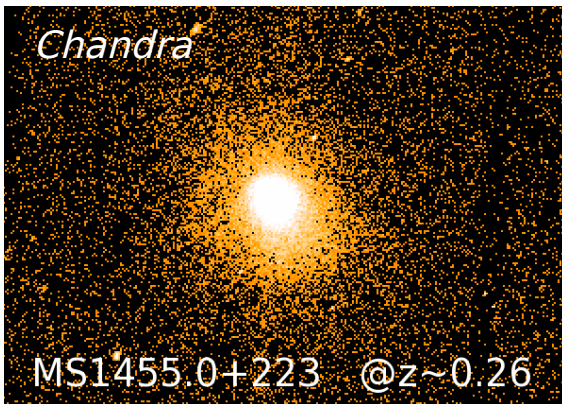
Red: model fit



X-ray emission

X-ray observations of high Z clusters suffer from cosmological dimming:

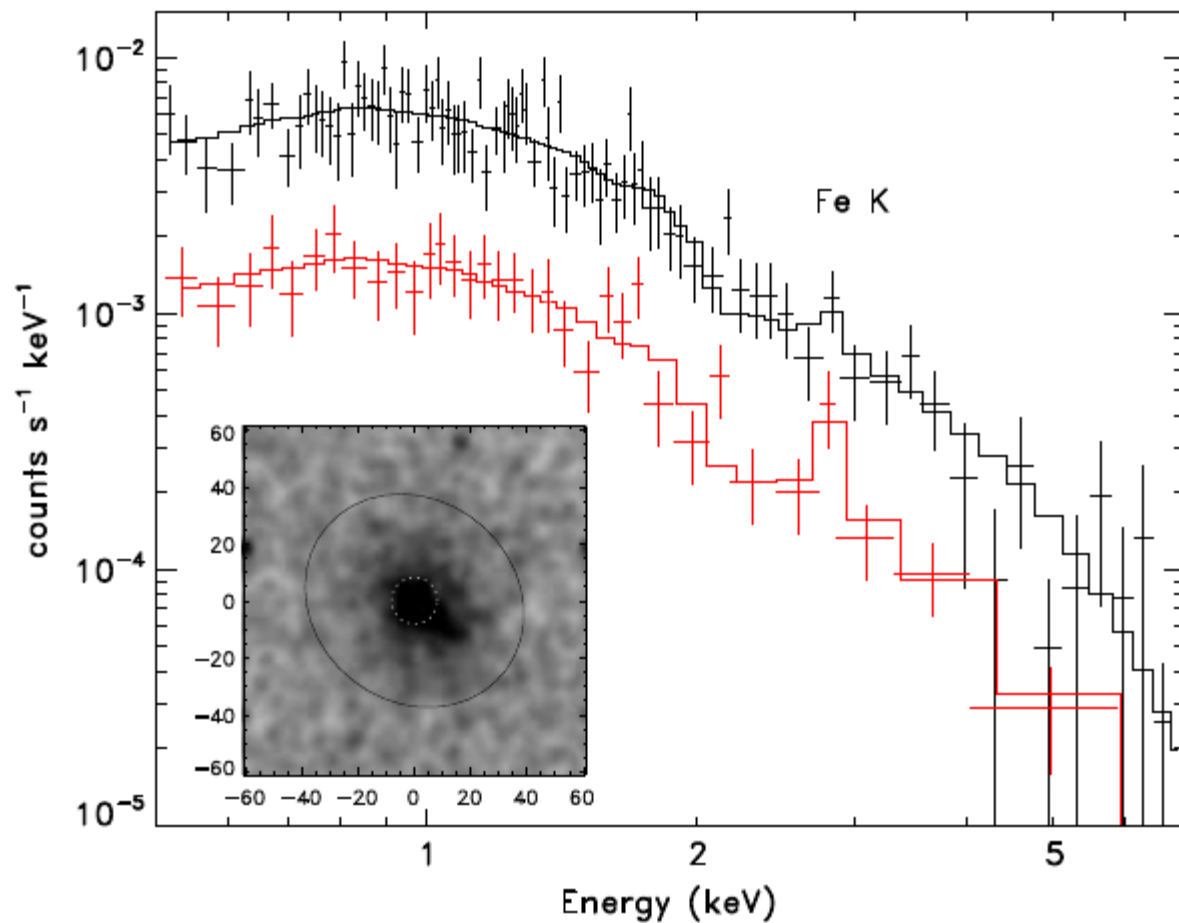
$$S_x \propto (1 + z)^{-4}$$



X-ray emission

200 ksec of Chandra
observation

Very massive system:
 $M_{200} = 6 \times 10^{14} M_{\text{sun}}$ at $z = 1.39$



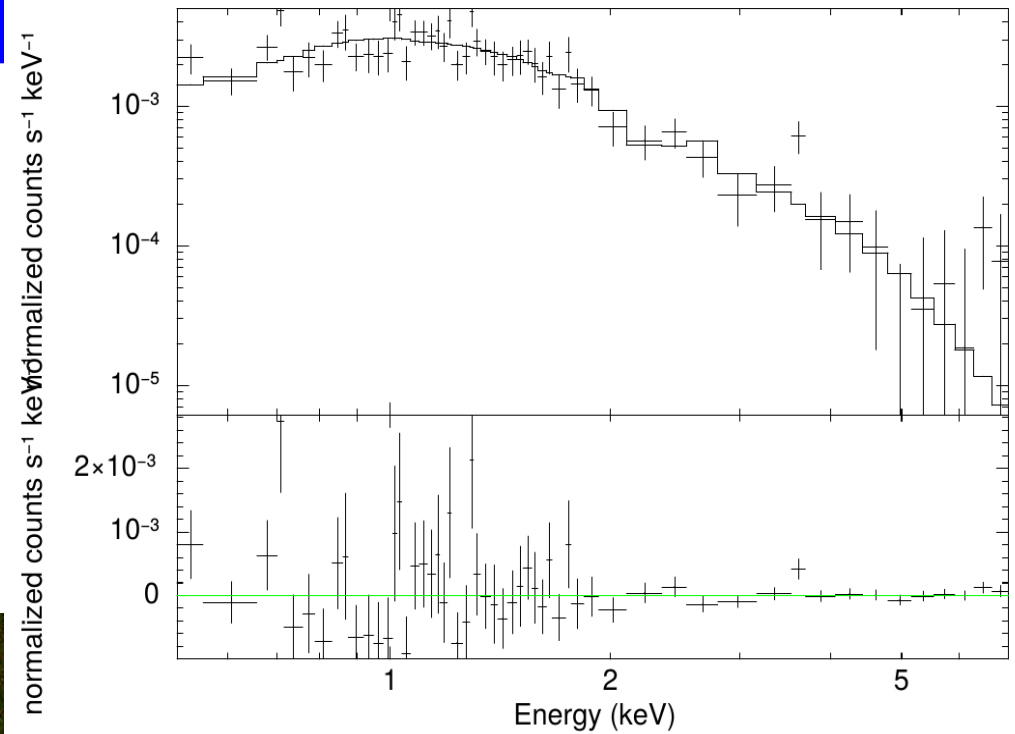
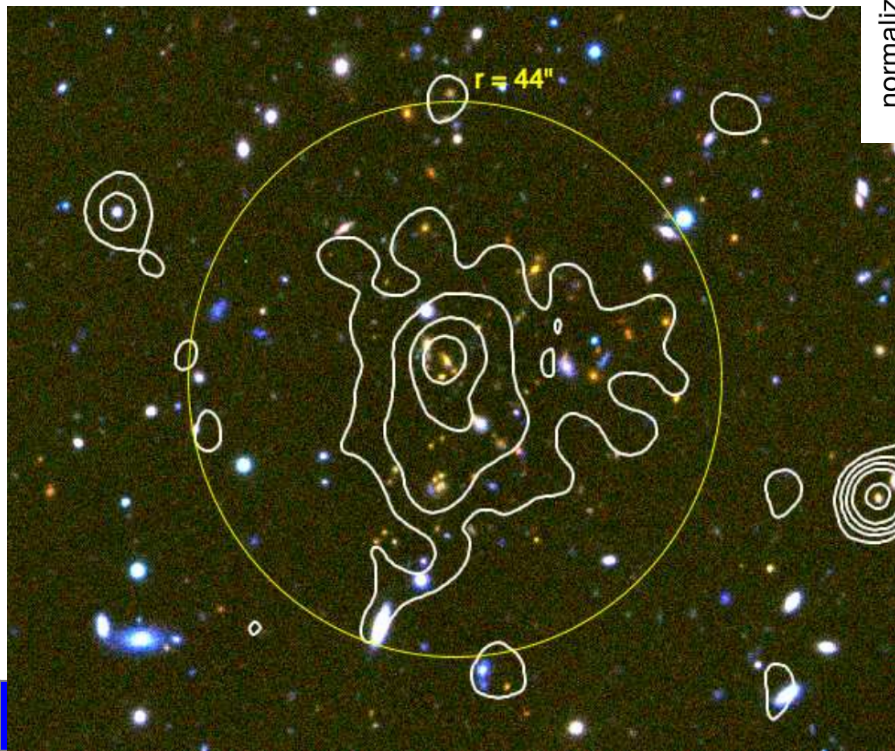
XMMUJ 2235.3 - 2033

Rosati et al. 2009

X-ray emission

380 ksec of Chandra
observation

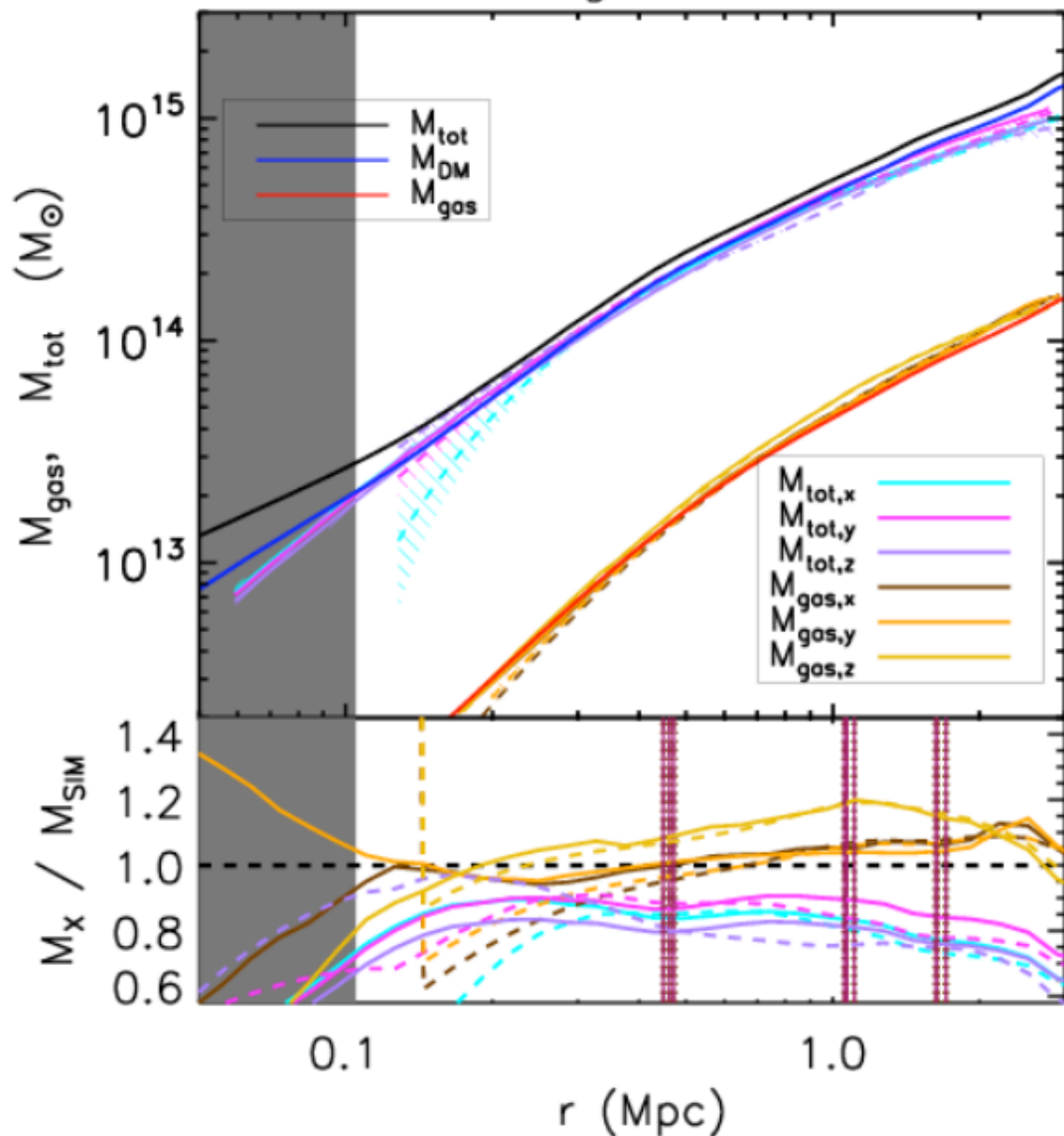
Very massive system:
 $M_{200} \sim 5 \times 10^{14} M_{\text{sun}}$ at $z=1.58$



XDCP0044

Tozzi et al. 2015

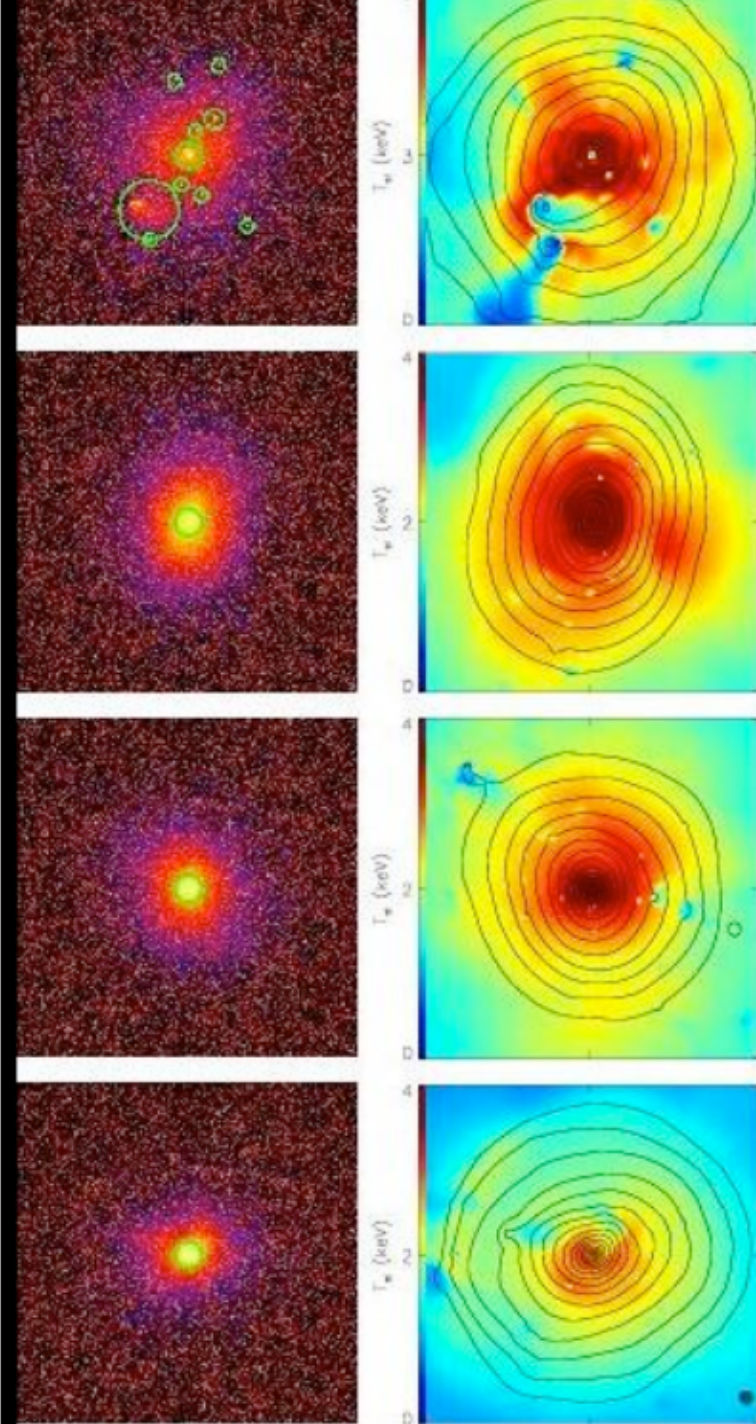
Different method to estimate the cluster mass from X-ray



Forward/backward methods (solid/dashed lines) are consistent within 10-15%

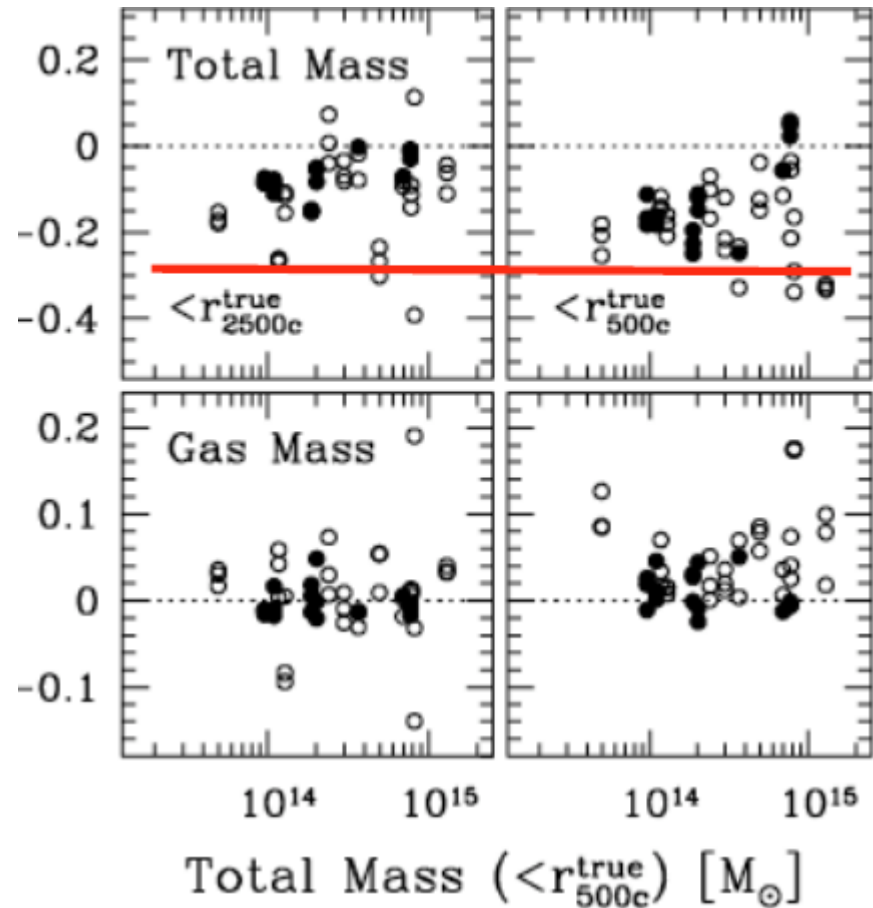
Systematics in Mass Estimation

5 clusters in different dynamical state have been extracted from simulation and processed to obtain mock Chandra (ACIS-S3) long (1 Ms) observations

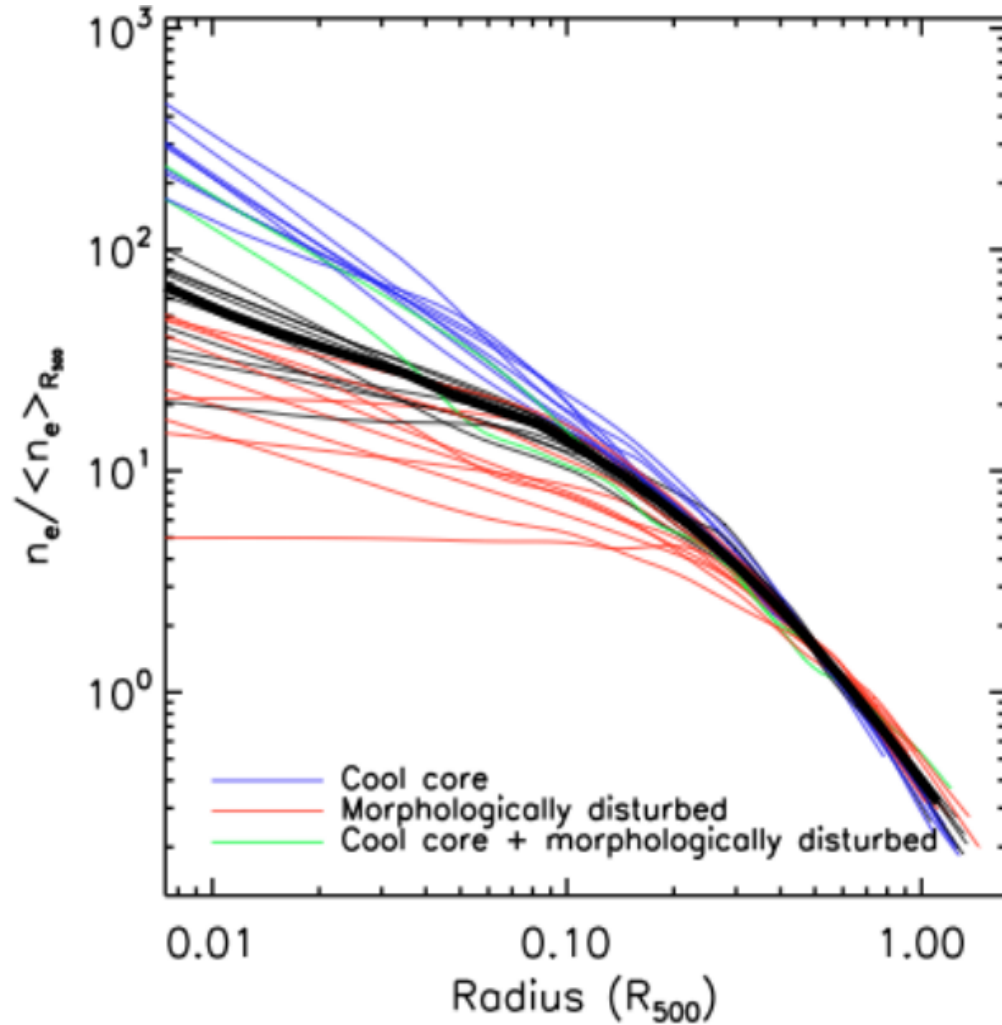


Systematics in Mass Estimation

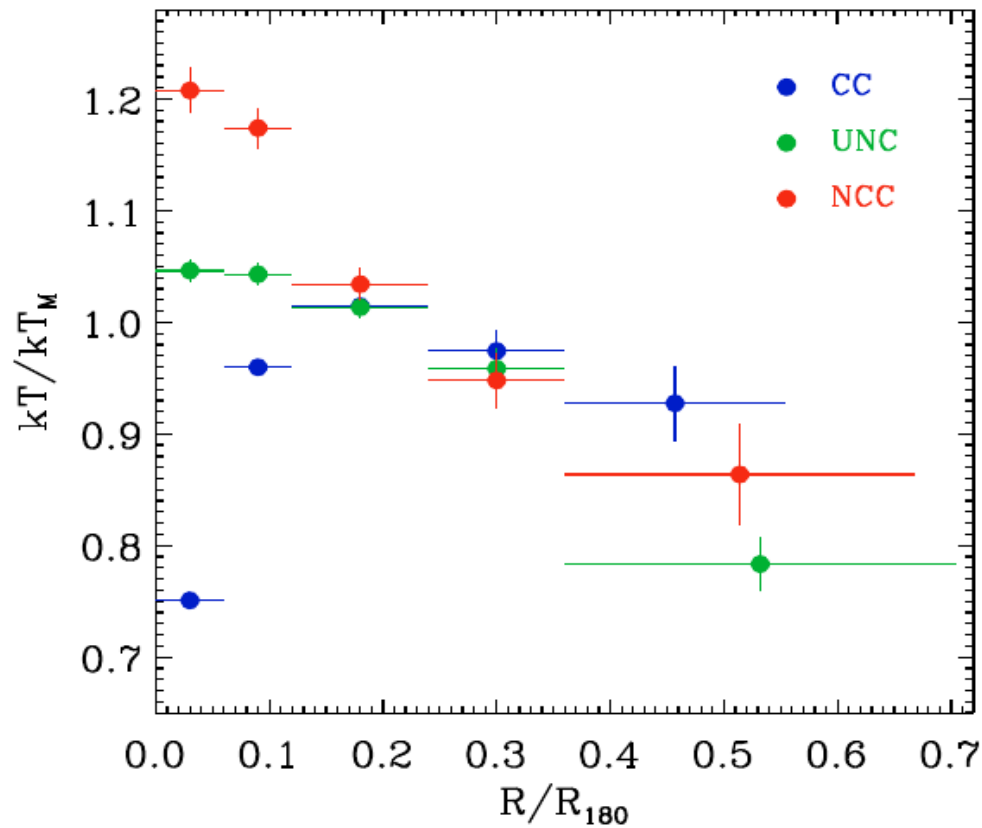
Ignoring the dynamical state of the cluster



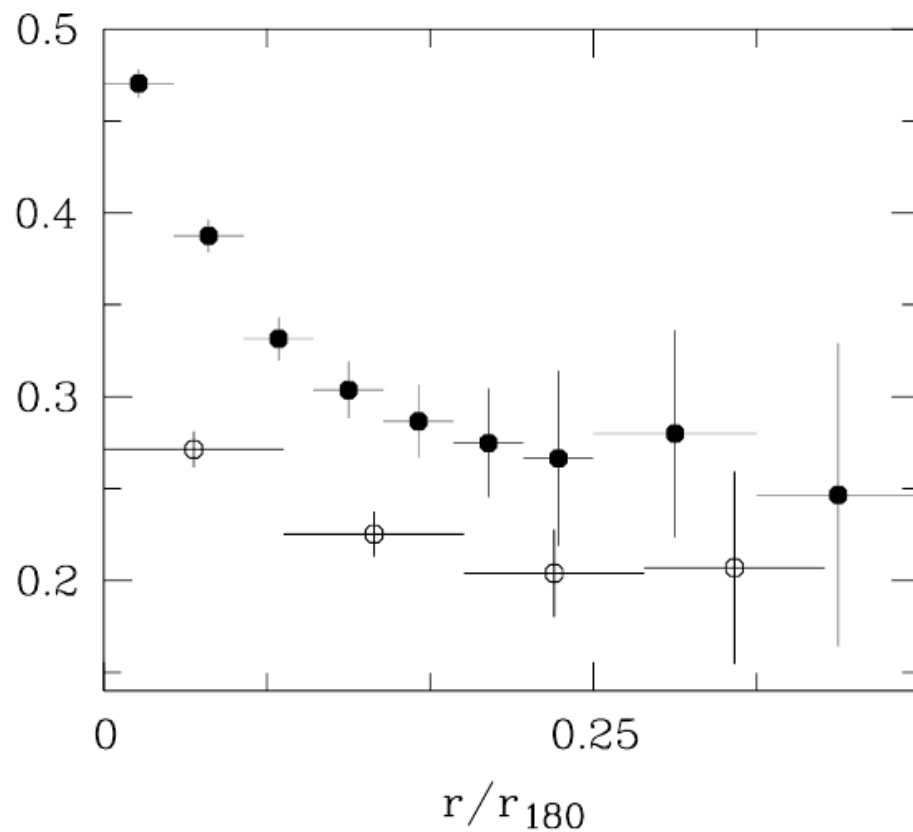
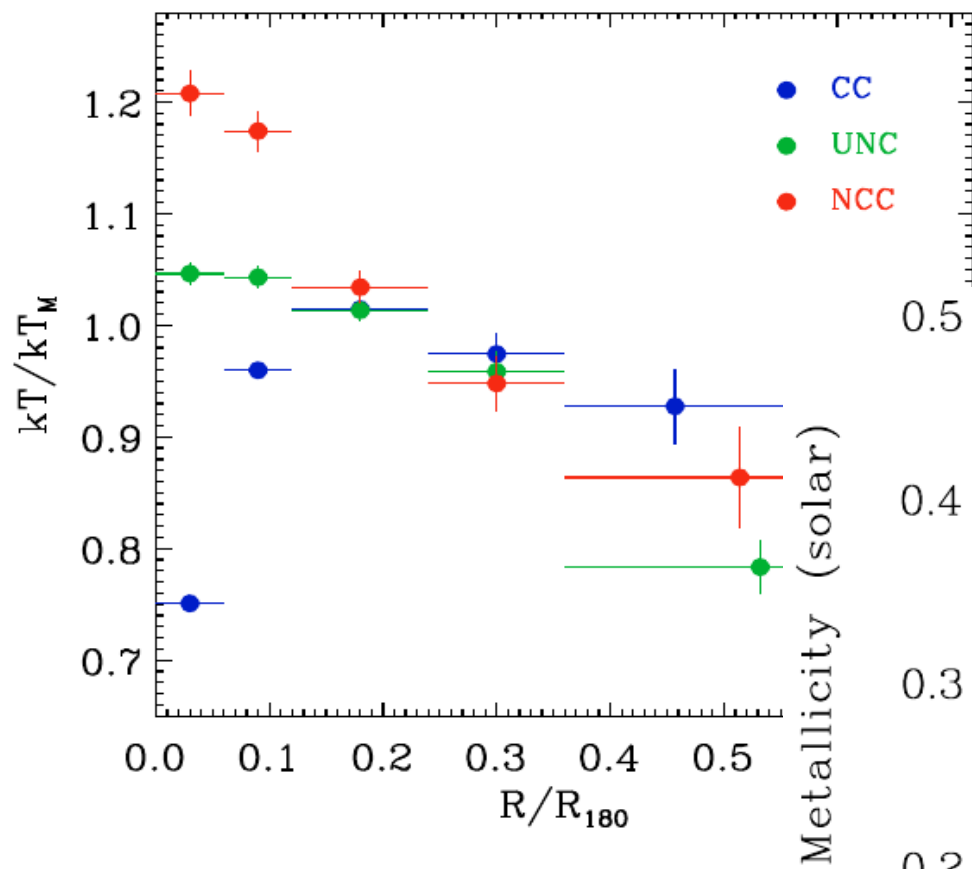
Cool core and non cool core clusters



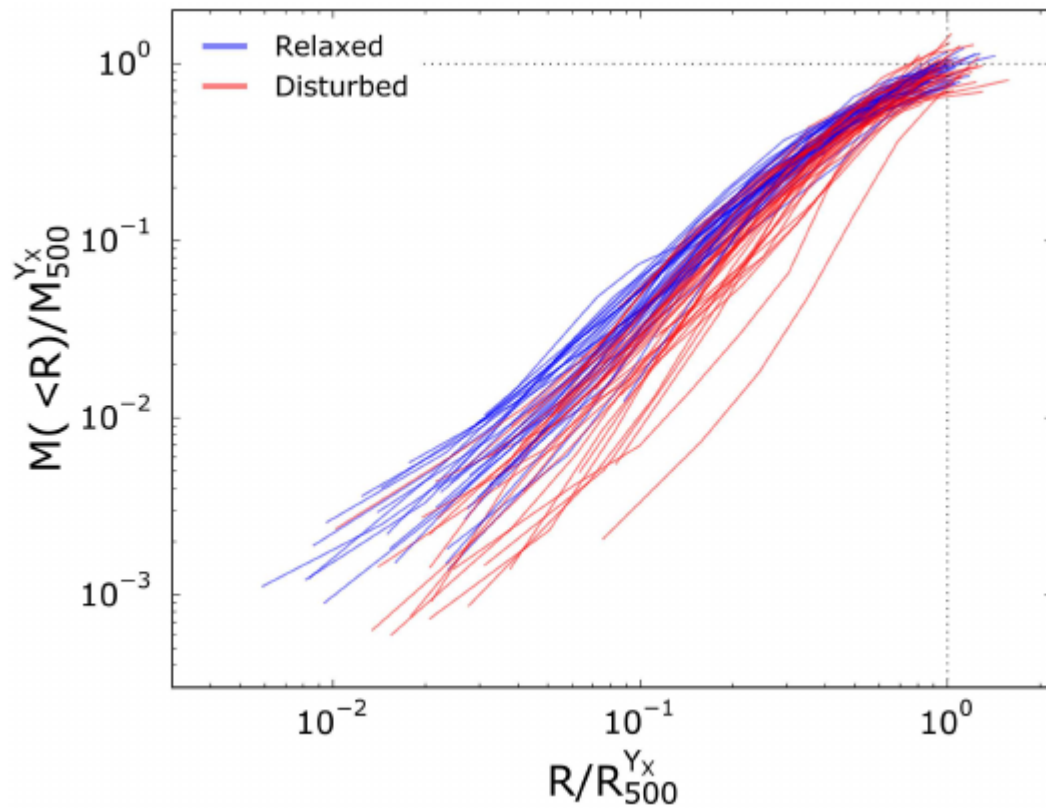
Cool core and non cool core clusters



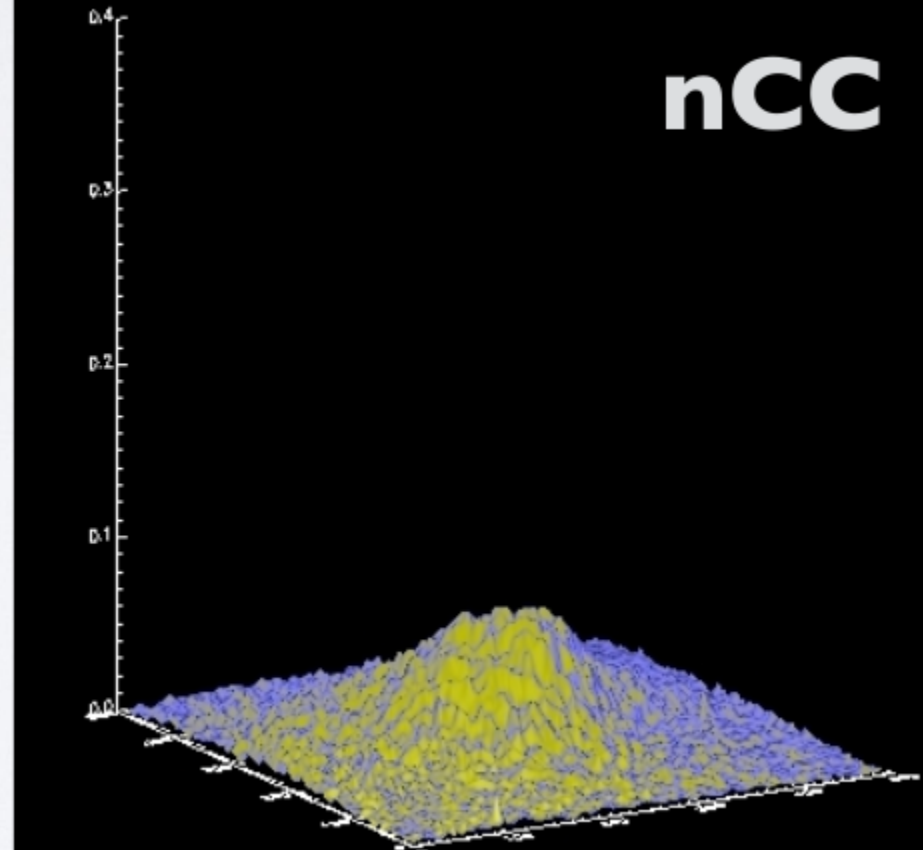
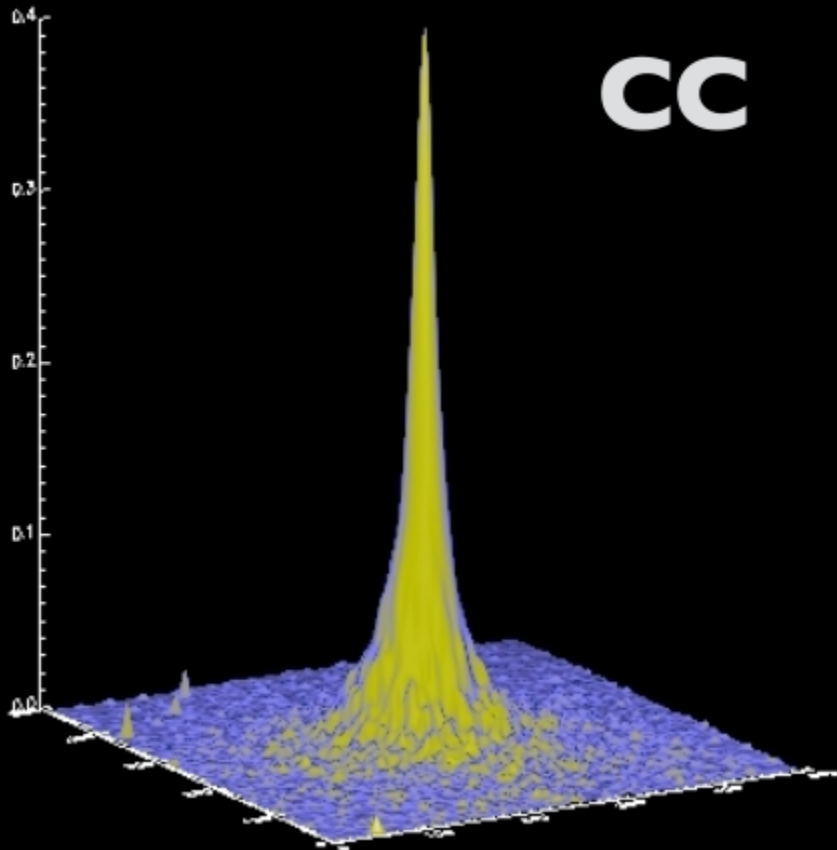
Cool core and non cool core clusters



Cool core and non cool core clusters



Cool core and non cool core clusters



X-ray telescopes

CHANDRA(NASA)



- Angular resolution: ~ 0.5 arcsec
- Energy range: [0.5-9] Kev
- Fov: ~ 16 arcmin

XMM-NEWTON(ESA)

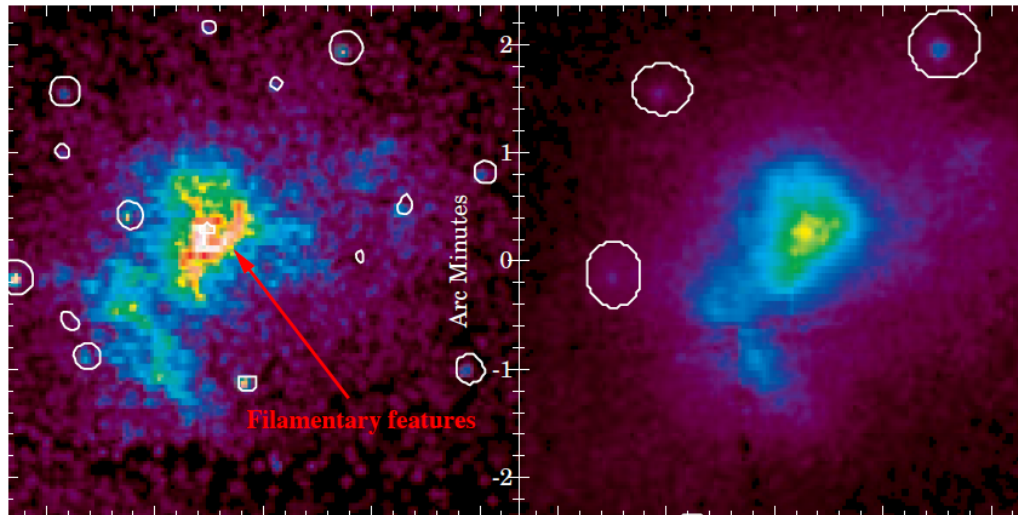


- Angular resolution: ~ 6 arcsec
- Energy range: [0.3-10] Kev
- Fov: ~ 30 arcmin

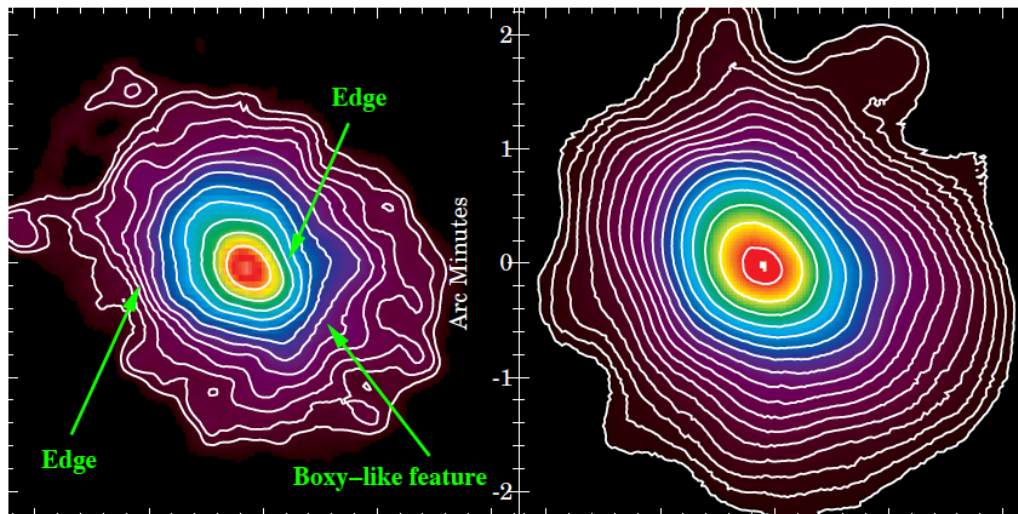
Instruments comparison

CHANDRA

XMM-NEWTON



MACS J0717.5+3745
 $Z = 0.55$



Cl0016+16
 $Z = 0.55$

X-ray event file

Both Chandra and XMM observations are available as a list of *events*, where an event is a list of informations for each detected photon.

XMM-NEWTON event file

	TIME	RAWX	RAWY	DETX	DETY	POS(X)	POS(Y)	PHA	PI	FLAG	PATTERN	CCDNR
units	s	PIXELS	PIXELS	pixel	pixel	pixel	pixel	CHAN	CHAN			
1	395587468.4	350	119	1084	-3995	26064	22332	3990	13069	4194304	0	1
2	395587468.4	570	164	5928	-3004	22021	19486	3989	13095	4194304	0	1
3	395587469.7	586	216	6281	-1865	20950	20010	3992	13118	4194304	0	1
4	395587468.2	511	242	4642	-1283	21650	21602	120	393	0	0	1
5	395587470.0	203	254	-2156	-1015	26117	26733	443	1477	0	0	1
6	395587472.1	366	399	1447	2175	21325	26299	425	1422	0	4	1
7	395587474.8	274	201	-592	-2198	25905	24784	520	1771	0	0	1
8	395587474.2	190	246	-2425	-1202	26438	26801	384	1274	0	0	1

time

position

energy

pattern

...plus a number of other files necessary for the calibration, sky projection ecc.

Chandra data archive:
wxc.cfa.harvard.edu/cda/

XMM-NEWTON data archive:
www.xmm.esac.esa.int/xsa/

Background

X-Ray background is formed by two main components:

Sky

- Local Hot Bubble and Trans absorption emission (e.g. Kuntz & Snowden 2000) modelled with two absorbed thermal emission

- Unresolved X ray point sources modelled with an absorbed power law (e.g. Lumb et al. 2002)

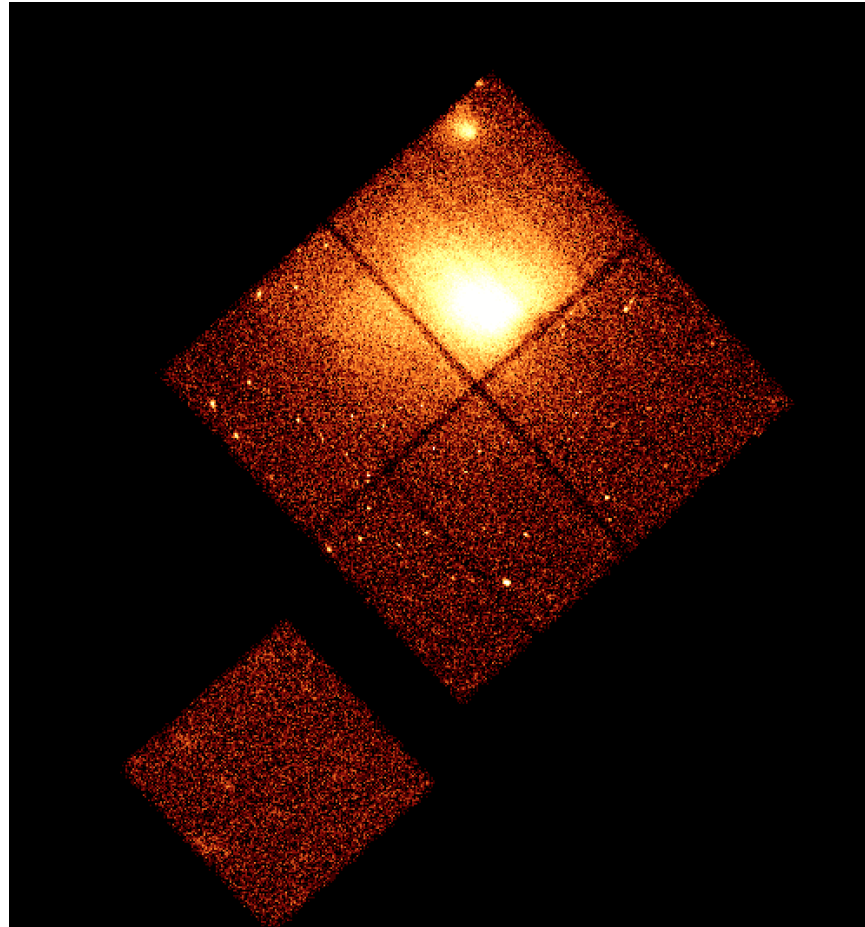
Instrumental

- Emission from telescope itself hit by high energetic particles(e.g. Hickox and Markevitch 2006)

- Particle revealed by the detectors as photons

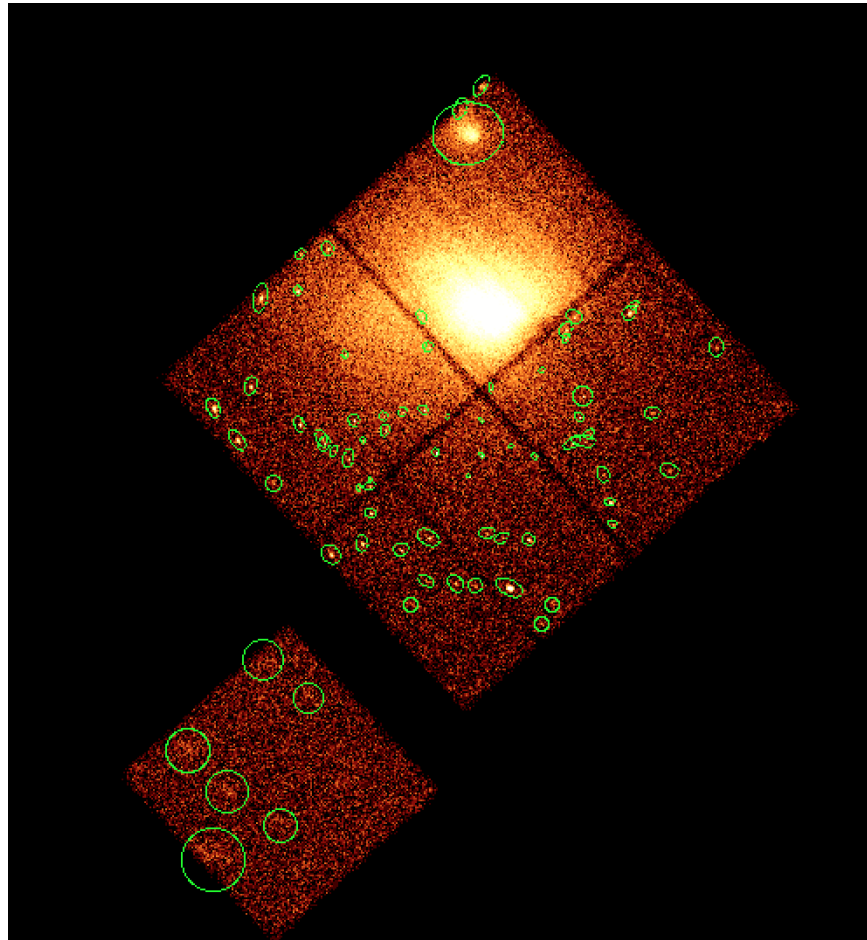
Source Detection

Remove photons coming from unwanted sources



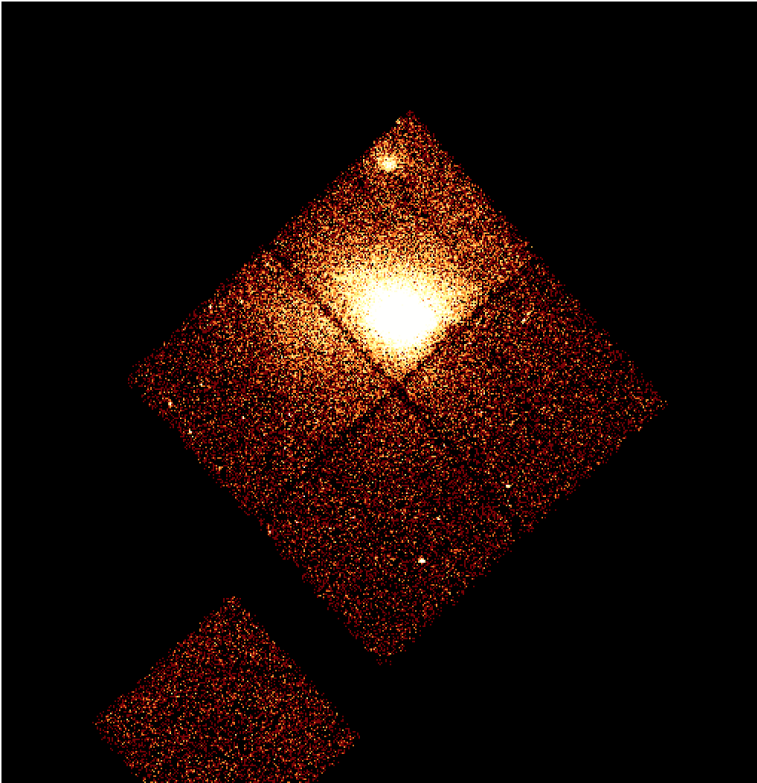
Source Detection

Remove photons coming from unwanted sources

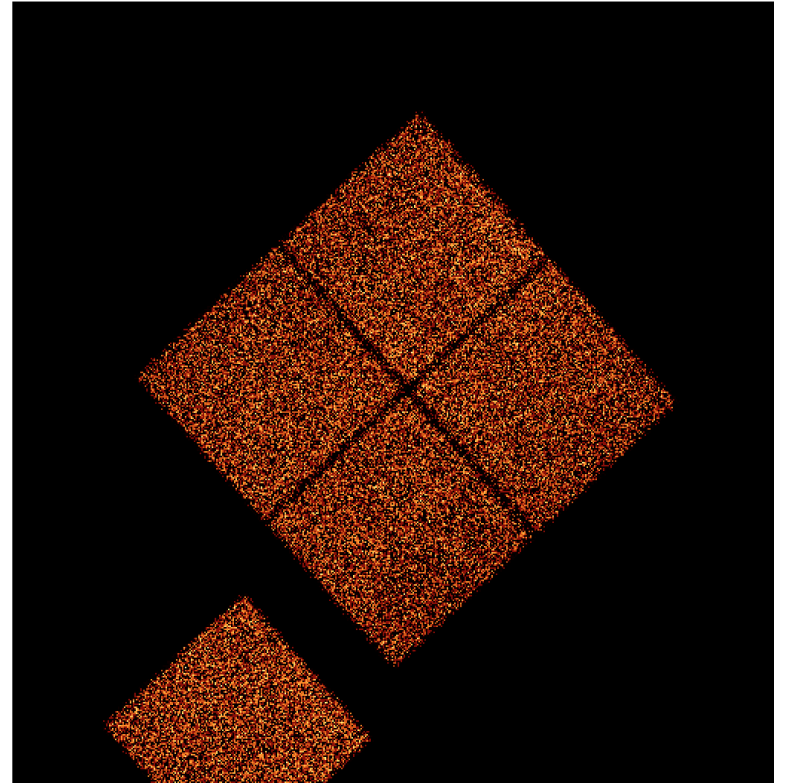


Background analysis

Cluster

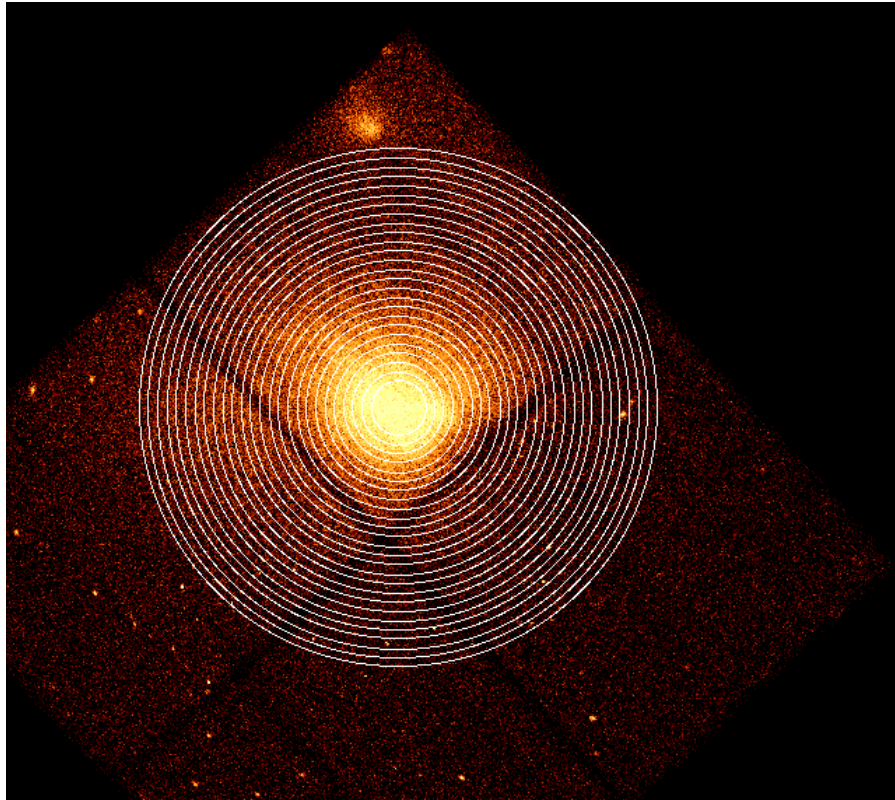


Background

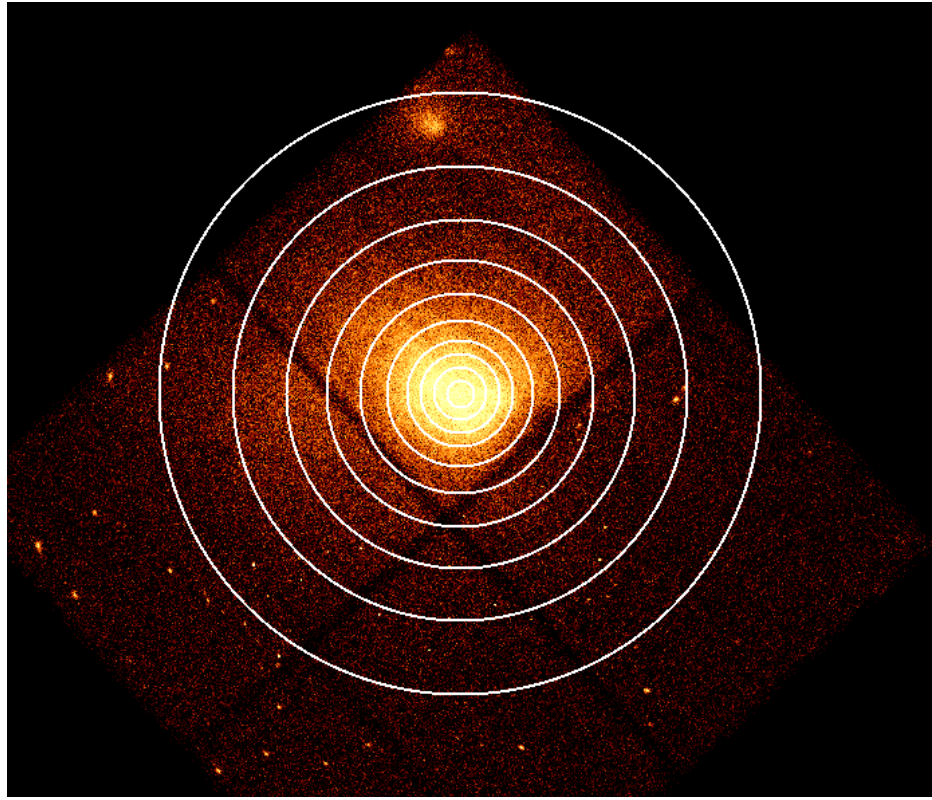


Spherical symmetry

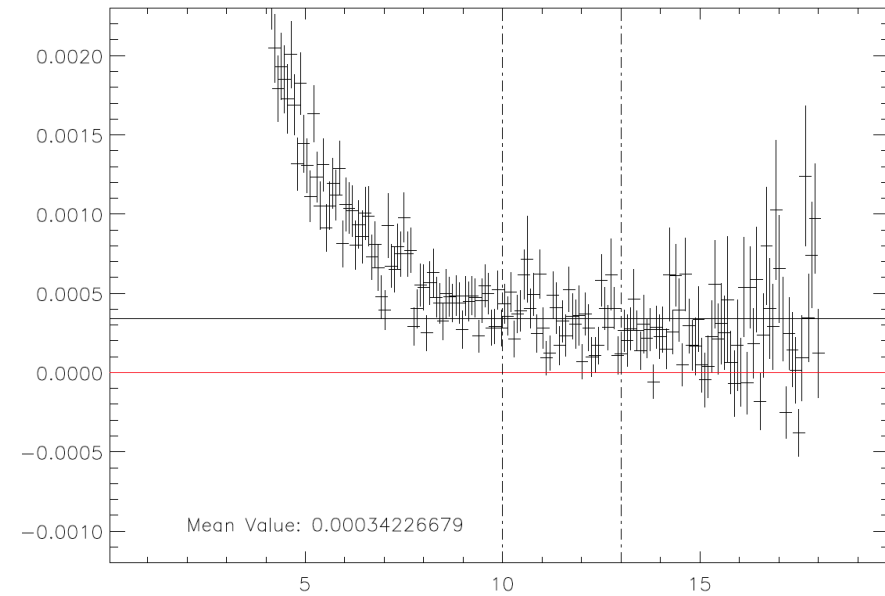
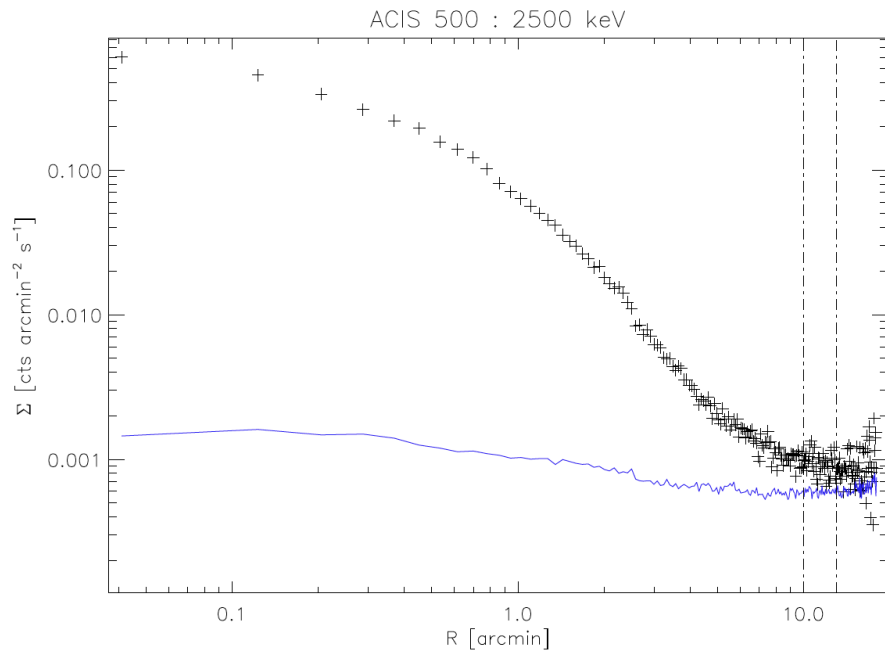
Surface brightness(S_x)



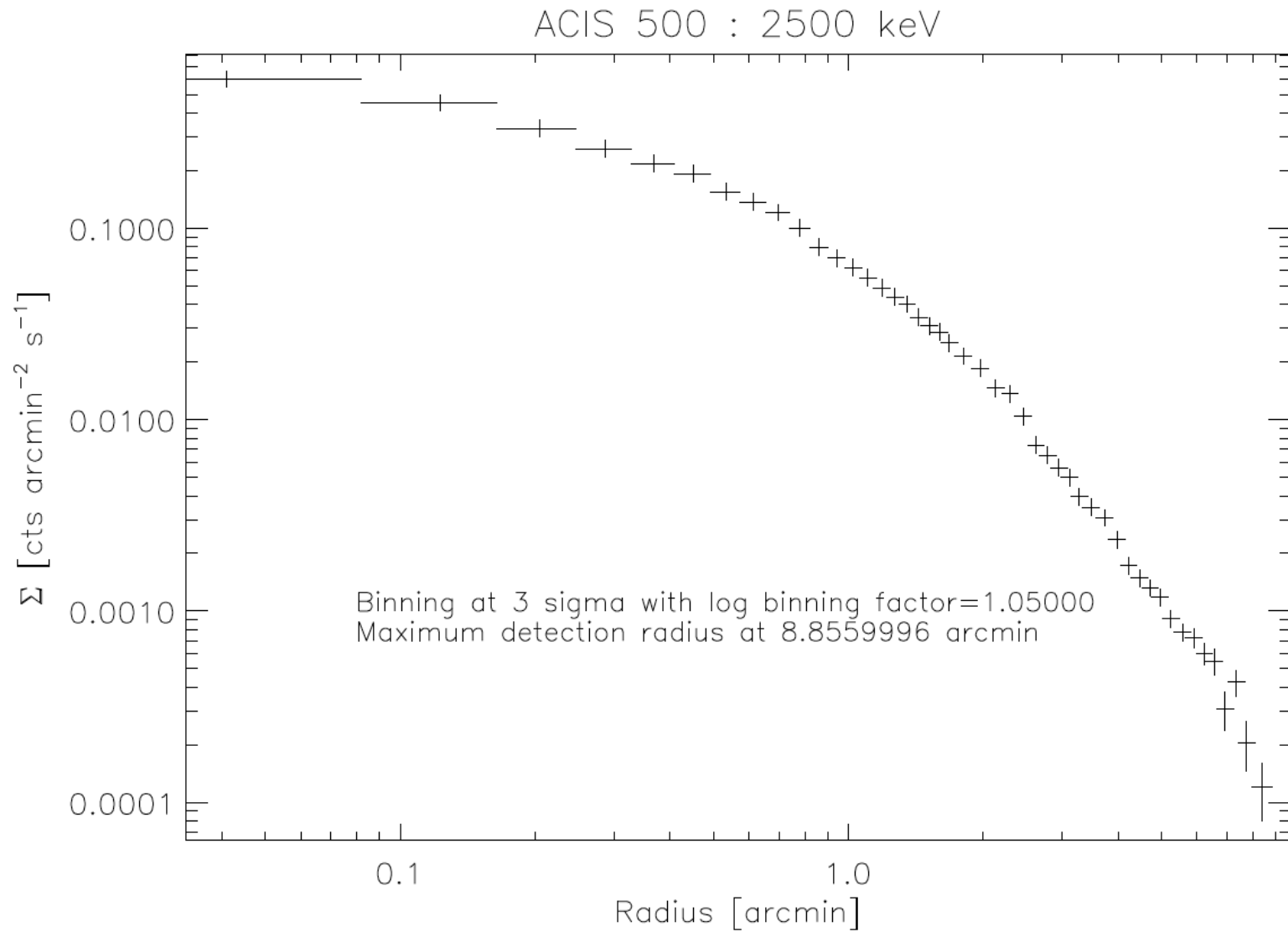
Temperature



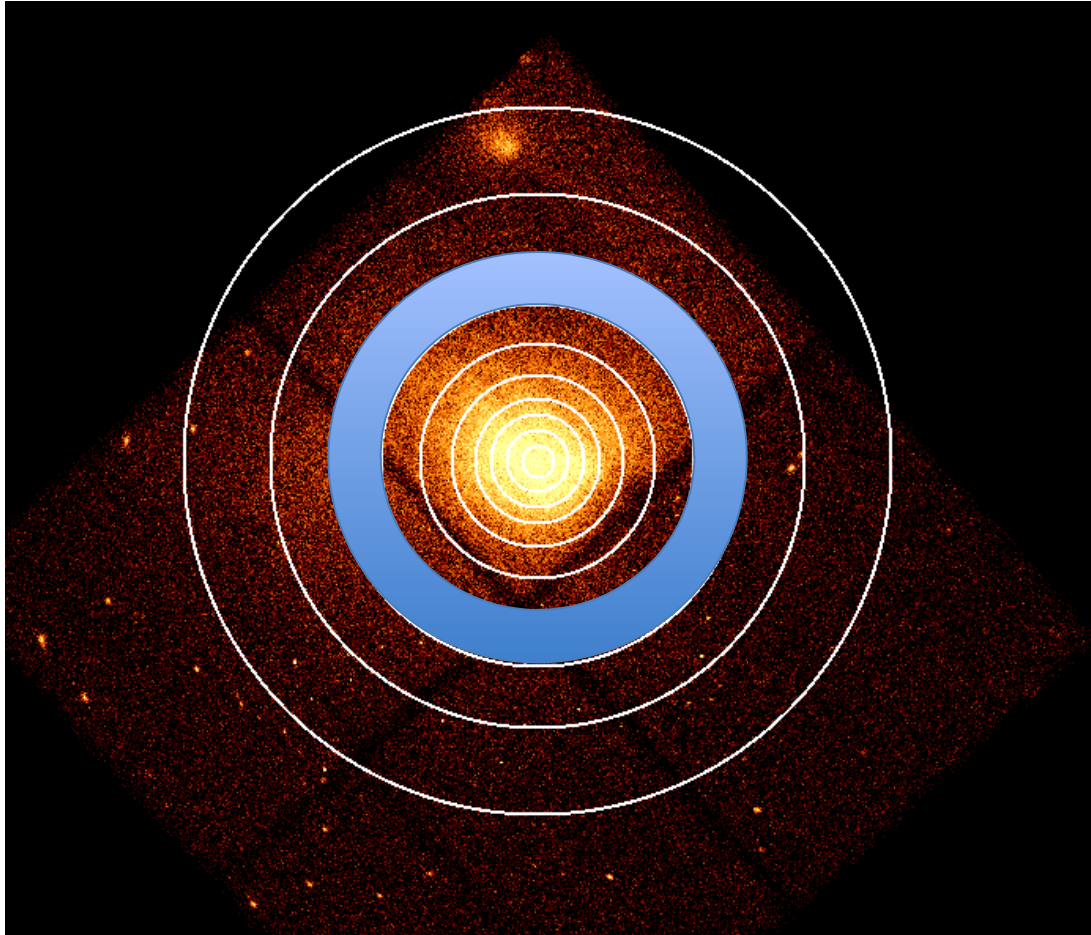
Surface brightness



Surface brightness

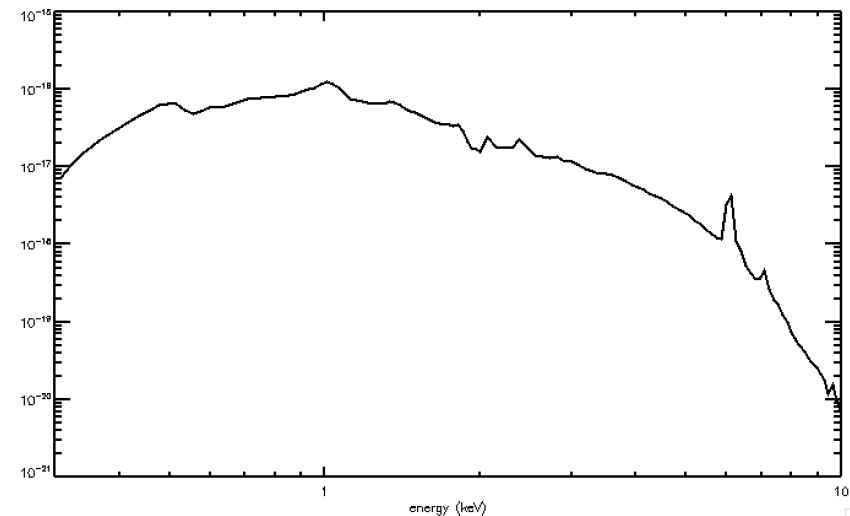
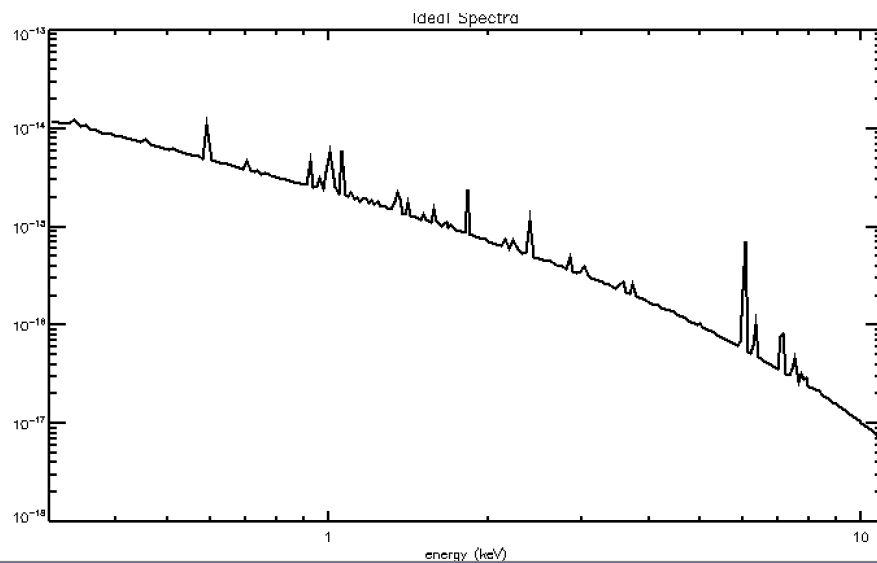


Temperature fit

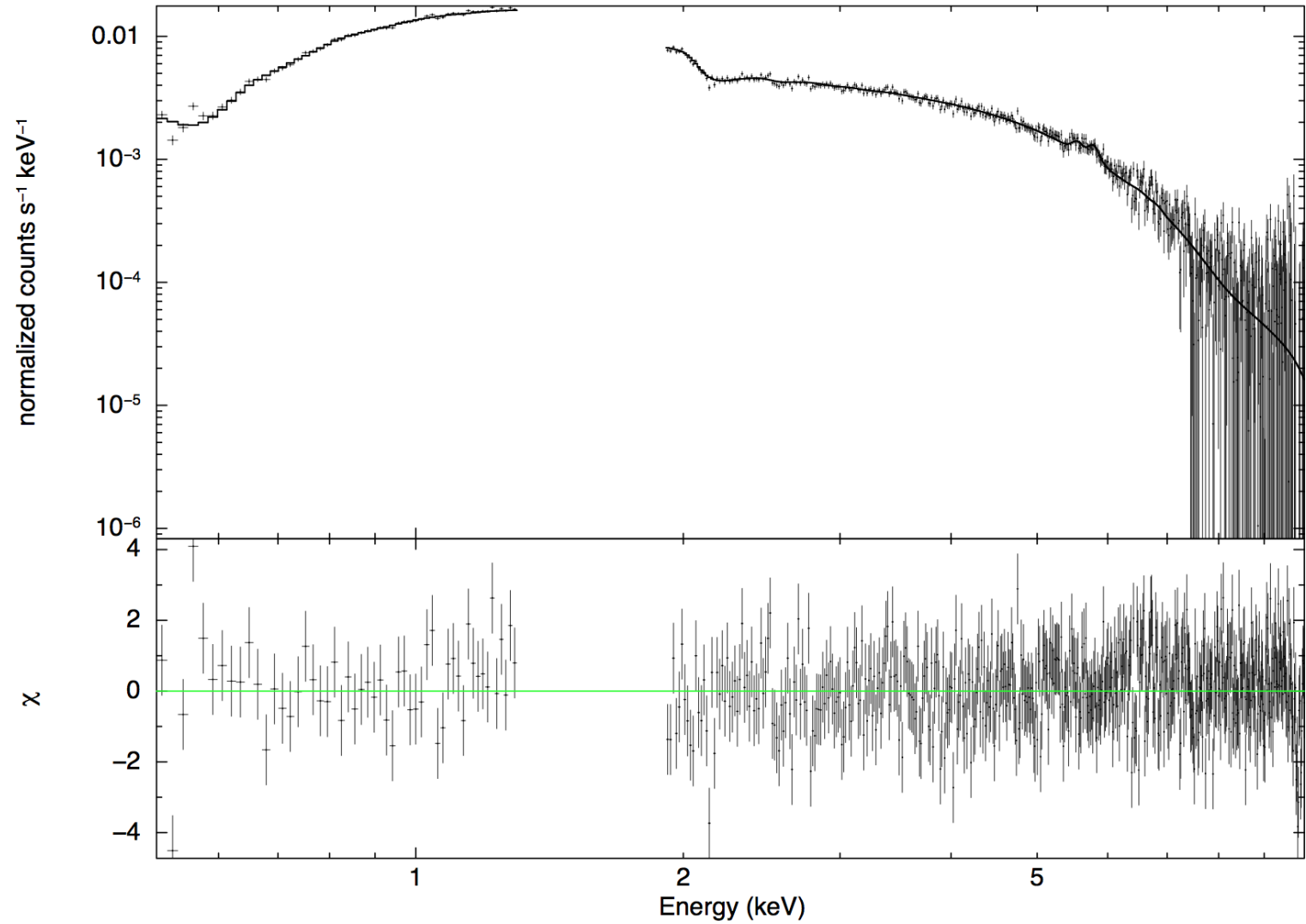


Instrumental effects: Temperature

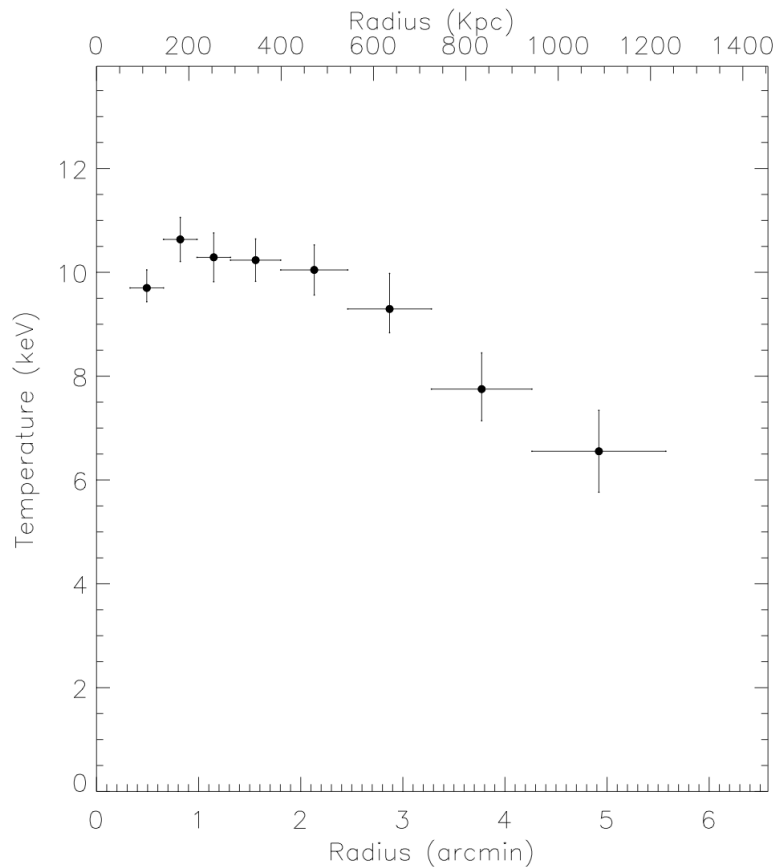
To estimate the temperature we fit data with tabulated spectral emissions in each bin convolved with instrument response, using the maximum likelihood method.



Temperature fit

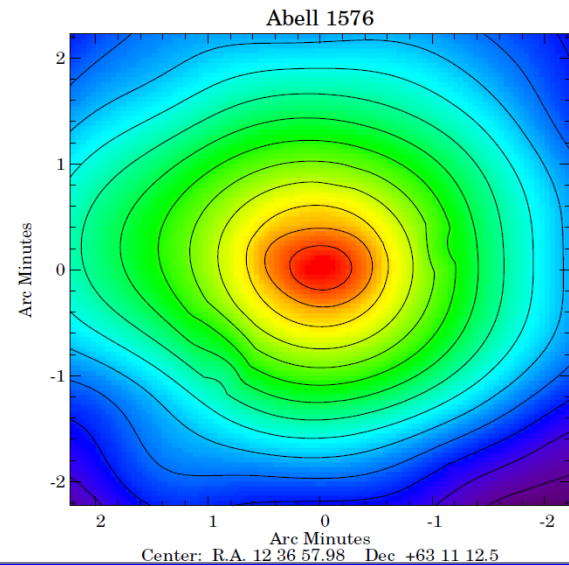
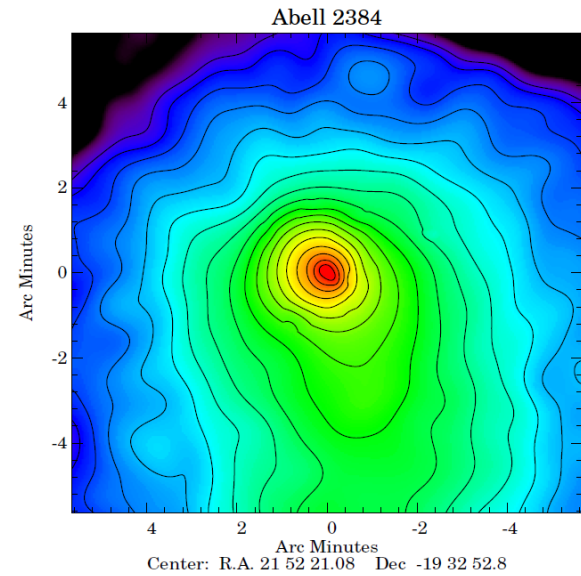
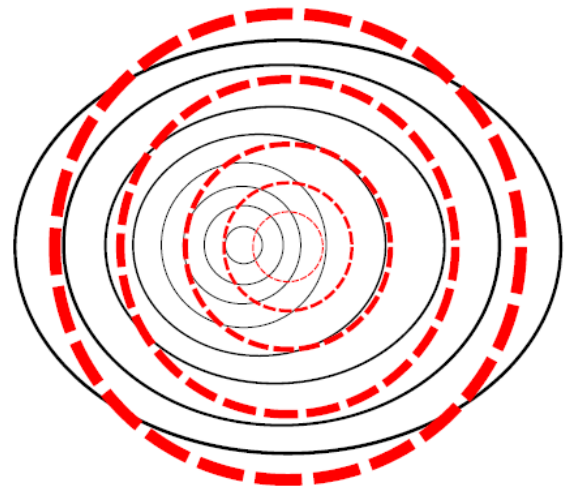
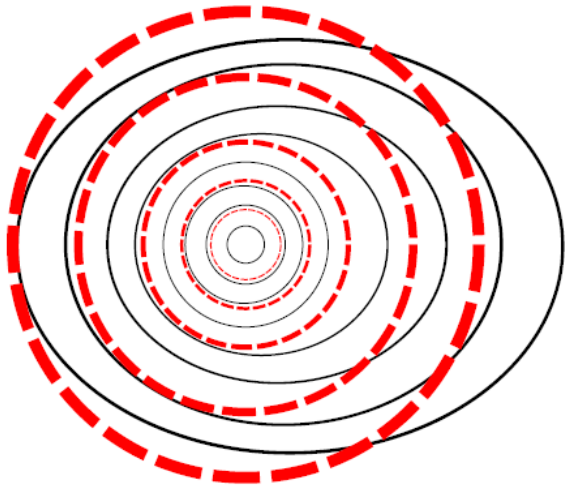


Temperature fit

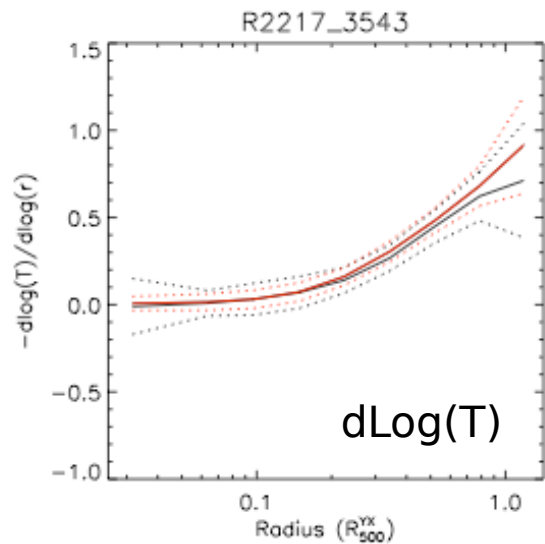
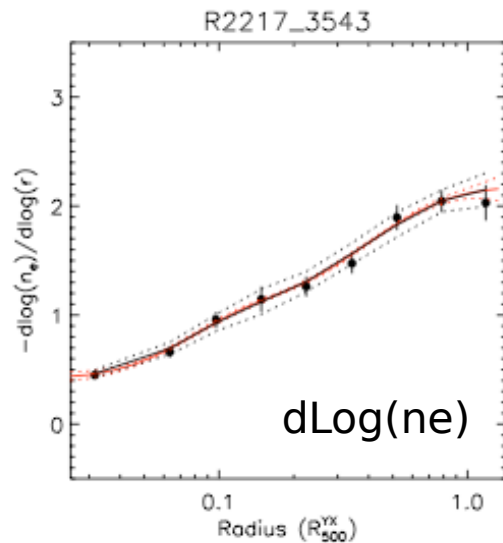


The observed emission is due to the superimposition of different radius at different temperatures. Projection effects should also be considered in the de-projection of the 2D temperature profile

Centroid or X-ray peak?



Mass derivation



$$M(r) = -\frac{kT r}{G\mu m_p} \left[\frac{d \log n_e}{d \log r} + \frac{d \log T}{d \log r} \right]$$

HE
→

